Interplay between T3SS effectors, ExoY activation, and cGMP signaling in *Pseudomonas aeruginosa* infection

Vincent Deruelle[1,*], Gabrielle Dupuis[1,3], Dorothée Raoux-Barbot[1], Elysa Lim[1,4], Roberto Ponce-López[1], Daniel Ladant[1], Louis Renault[2] and Undine Mechold[1,5,**]

[1]Institut Pasteur, Université Paris Cité, CNRS UMR3528, Biochemistry of Macromolecular Interactions Unit, Paris, France

[2]Université Paris-Saclay, CEA, CNRS, Institute for Integrative Biology of the Cell (I2BC), Gif-sur-Yvette, France

[3]Centre de Recherche Saint-Antoine (CRSA), Sorbonne Université, INSERM UMR S 938, 5PMed : Pulmonary diseases, Pathogens, Physiopathology, Phenogenomics and Personalized Medecine, Paris, France

[4]Present address: School of Biomolecular and Biomedical Science and Michael Smurfit Graduate Business School, University College Dublin, Ireland

[5]Lead contact

* Correspondence: vincent.deruelle@pasteur.fr

** Correspondence: undine.mechold@pasteur.fr

ABSTRACT

ExoY is a nucleotidyl cyclase, secreted by the *Pseudomonas aeruginosa* type 3 secretion system (T3SS), which generates various cyclic nucleotides within host cells, predominantly cGMP. How ExoY-catalyzed cNMPs production contributes to the infection process remains unclear. Using recombinant *P. aeruginosa* strains expressing ExoY variants with different substrate specificities, we identified that ExoY-derived cGMP modulates the cytotoxicity of ExoT, a co-injected T3SS exotoxin. Our results demonstrated that dephosphorylation of the host CrkII adaptor protein, a downstream effect of the ADP-ribosyltransferase activity of ExoT, is limited by ExoY-derived cGMP, therefore antagonizing ExoT-induced cell retraction. We also revealed a reciprocal interaction between T3SS effectors, showing that ExoT and ExoS, can in turn, suppress ExoY activity and its production of cGMP in certain cell types, thereby limiting their regulation by ExoY-synthesized cGMP. These findings highlight the intricate interplay between T3SS effectors and uncover a novel host cell-dependent regulation within *P. aeruginosa* infections.

31 **INTRODUCTION:**

32 *Pseudomonas aeruginosa* is a highly adaptable Gram-negative opportunistic pathogen
33 that infects a wide range of hosts. In humans, *P. aeruginosa* is a major cause of nosocomial
34 infections, leading to acute or chronic life-threatening infections[1,2]. Lung infections caused by
35 *P. aeruginosa* are particularly common in hospitalized patients, with clinical outcomes ranging
36 from rapidly fatal pneumonia in immunocompromised patients to long-term bronchitis in
37 cystic fibrosis (CF) patients[3–6]. The type 3 secretion system (T3SS) plays a key role in *P.*
38 *aeruginosa* pathogenicity and its expression is associated with severe clinical outcomes and
39 increased mortality[7–9]. This system delivers four effectors, ExoS, ExoT, ExoU and ExoY, directly
40 into the host cell's cytosol[10], where they are activated by specific host factors[11–14]. Most strains
41 inject up to three exotoxins simultaneously. ExoS and ExoU were previously thought to be
42 mutually exclusive[15,16], but recent findings have shown that some clinical isolates carry both
43 genes and express them jointly, resulting in significantly enhanced virulence[17–19]. Initially
44 identified as a T3SS effector with adenylate cyclase activity[20], ExoY was later characterized as
45 a nucleotidyl cyclase (NC) with broad substrate specificity[21,22]. In host cells, ExoY is activated
46 by F-actin[14,23–26] and promotes the accumulation of various cyclic nucleotide monophosphates
47 (cNMPs), favoring cyclic guanosine monophosphate (cGMP) and cUMP rather than cAMP and
48 cCMP[27]. *In vitro*, the substrate's preference of ExoY follows: GTP > ATP ≥ UTP > CTP[22],
49 distinguishing it from ExoY-like orthologs and the structurally-related NC toxins EF from
50 *Bacillus anthracis* and CyaA from *Bordetella pertussis*, which prefer ATP[22,27,28].

51 The high prevalence of the *exoY* gene (89–100% of strains) and secretion of the protein
52 across diverse isolates[15,17,29–31] suggest that ExoY is a key component of *P. aeruginosa*
53 virulence. However, compared to ExoS, ExoT and ExoU that are known to directly induce cell
54 death and facilitate infection, ExoY's role in *P. aeruginosa* pathogenicity remains controversial,
55 according to different studies using distinct experimental conditions [21,32–40]. ExoY has been
56 either studied using bacteria with a native expression level or with bacteria that overexpress
57 ExoY from a multi-copy plasmid, therefore modifying the levels of injected ExoY[41]. Co-injected
58 effectors can also act synergistically[42] thus adding to the complexity, and ExoY has for instance
59 been suggested to play a protective role under some conditions by attenuating the
60 cytotoxicity of ExoS and ExoT [30,43].

61 The aim of this study is to investigate the contribution of ExoY-catalyzed cNMPs in the
62 infection process, with a particular focus on cGMP, the predominant cNMP produced by ExoY.
63 We therefore constructed genetically modified *P. aeruginosa* strains expressing ExoY variants
64 with different substrate specificities. This modification allowed us to identify a specific role for
65 cGMP, and to uncover the mechanism underlying ExoY's antagonistic effect on ExoT
66 cytotoxicity. Additionally, we found that ExoS or ExoT activities can counteract ExoY activation
67 depending on the infected cell type, further emphasizing the intricate interplay among T3SS
68 effectors in infected cells.

69 **RESULTS**

70 **Modification of the ExoY nucleotide-binding pocket to change substrate specificity**

71 To investigate the role of ExoY-catalyzed cGMP production in infected cells, we engineered
72 ExoY variants with altered nucleotide triphosphate (NTP) specificities, in order to shift
73 substrate preference from GTP to ATP. Based on the recently solved structure of ExoY, we
74 identified residues in the nucleotide-binding pocket potentially involved in GTP specificity[23]
75 (Figure 1A). These residues were replaced with those from structurally-related nucleotidyl
76 cyclases (NCs) with narrower substrate specificities, such as the adenylate cyclase toxins from
77 *Bordetella pertussis* (CyaA) and *Bacillus anthracis* (EF), or the ExoY-like modules from *Vibrio*
78 *vulnificus* and *V. nigripulchritudo*[14,22,23] (Figure S1). Consequently, three ExoY variants were
79 designed: ExoY^{mut1} (N264V, F289V, S292G and D293A, one letter code for amino acids),
80 ExoY^{mut2} (F83L and S292G) and ExoY^{mut3} (F83L, E258D and S292G). The recombinant proteins
81 were expressed in *E. coli* and purified *via* an added C-terminal His-tag. The catalytic activities
82 of each variant were assessed *in vitro*, using the purified proteins in the presence of the F-
83 actin activator and radioactive GTP, ATP, UTP or CTP as substrate, and then compared to WT
84 ExoY to illustrate the change in substrate specificity (Figures 1B-1E). A catalytically inactive
85 mutant, ExoY^{mut0} (K81M and K88I)[22] served as a negative control. As shown in Figure 1,
86 ExoY^{mut1} exhibited a drastic reduction in cGMP and cUMP synthesis compared to WT ExoY but
87 maintained cAMP and cCMP production. Conversely, ExoY^{mut2} and ExoY^{mut3}, while retaining
88 wild type cUMP and cCMP production, produced significantly more cAMP than WT ExoY (38-
89 and 23-fold increases, respectively). In addition, ExoY^{mut3}, which contains the additional E258D
90 substitution compared to ExoY^{mut2}, showed a markedly reduced cGMP-synthetizing activity.

91 To confirm these biochemical data, we tested the substrate preferences of the mutants
92 when expressed in NCI-H292 cells, a human bronchial epithelial cell line previously used to
93 study *P. aeruginosa* infection[30]. For this, we cloned the WT and mutant *exoY* alleles into a Tet-
94 On 3G inducible expression plasmid, which enables a precise control of *exoY* transcription in
95 cells by doxycycline. In parallel, we also created stable reporter cell lines that allow
96 measurement of cGMP or cAMP accumulation by recording luminescence with the GloSensor
97 technology (Promega) (Figure S2A). Plasmids (encoding the Tet-On 3G transactivator and the
98 various *exoY* alleles) were therefore transfected into the cGMP/cAMP reporter cell lines to
99 measure the production of cGMP or cAMP. Luminescence in doxycycline-induced cells was

100 monitored and maximum values for each construct were plotted (Figures S2B–S2D). In the
101 cGMP reporter cell line, only ExoY and ExoY^{mut2} induced strong luminescence, while the
102 luminescence in cells expressing the ExoY^{mut1} and ExoY^{mut3} was comparable to that of cells
103 expressing the catalytically inactive ExoY mutant (ExoY^{mut0}) (Figures 1F). ExoY^{mut2} and ExoY^{mut3}
104 produced significantly higher luminescence in the cAMP reporter cell line as compared to ExoY
105 and ExoY^{mut1} (Figures 1G). Therefore, the cGMP/cAMP levels measured for the different ExoY
106 alleles in transfected cells appeared to be in excellent agreement with the *in vitro* activities of
107 the purified proteins.

108 Finally, we examined the cGMP/cAMP levels in cells infected with recombinant *P.*
109 *aeruginosa* strains expressing the different ExoY variants. To maintain native expression level,
110 we performed allelic exchange to replace the WT *exoY* allele and introduce mutations
111 corresponding to each ExoY variant into the genome of *P. aeruginosa* PAO1FΔExoS (PAO1F
112 strain secreting only ExoT and ExoY effectors). NCI-H292 cells were infected with these
113 recombinant strains and the intracellular production of cGMP and cAMP was measured using
114 ELISA kits (cUMP and cCMP could not be measured due to the lack of specific kits). Injection
115 of WT ExoY or ExoY^{mut2} resulted in a large increase in cGMP levels (Figure 1H). However, in
116 line with the experiments described above, injection of ExoY^{mut0}, ExoY^{mut1} and ExoY^{mut3}
117 effectors did not result in a detectable increase in cellular cGMP (i.e. similar to the uninfected
118 control). Regarding cAMP production in infected cells, only the injection of the ExoY^{mut2} or
119 ExoY^{mut3} variants, which have a higher adenylyl cyclase catalytic efficiency, produced
120 detectable cAMP in infected cells. Injection by bacteria of WT ExoY, ExoY^{mut0} and ExoY^{mut1}
121 effectors, did not yield measurable increases in cAMP as compared to uninfected cells (Figure
122 1I). The levels of cAMP produced by the injection of one of these three ExoY variants should
123 therefore be close to the detection limit of the cAMP ELISA kit.

124 In summary, these results demonstrate that the amino-acid substitutions introduced
125 into the ExoY nucleotide-binding pocket successfully altered substrate specificity, leading to
126 differential cNMP accumulation in cells. The substrate specificity of the WT and ExoY mutant
127 alleles, as derived from these results and summarized in Figure 1J, allowed us to further
128 investigate the physiological role of these different cyclic nucleotides in infected cells.

129 **In NCI-H292 cells, ExoY-derived cGMP dampens the cytotoxicity of ExoT but not that of ExoS**

130 ExoY is never injected alone into cells by the T3SS, but always co-injected with ExoT and/or
131 ExoS effectors. In contrast to ExoT and ExoS, ExoY does not exhibit detectable cytotoxicity *per*
132 *se*, when injected alone at physiological levels by bacteria harboring a single chromosomal
133 copy of the *exoY* gene[29,30,44]. ExoY was even suggested to exert a protective role by attenuating
134 the cytotoxicity of ExoT and ExoS[30,43]. Since ExoY produces diverse cNMPs in cells, we
135 wondered which of these cNMPs could be implicated in the modulation of cytotoxicity
136 induced by ExoT or ExoS. We therefore introduced the various *exoY* alleles into the genome
137 of the *P. aeruginosa* PAO1FΔS (secreting only ExoT and ExoY effectors) and PAO1FΔT
138 (secreting only ExoS and ExoY effectors) strains. The resulting strains thus produced the
139 different ExoY variants (or WT) and either ExoT (PAO1FΔS derivatives) or ExoS (PAO1FΔT
140 derivatives). These strains were then compared in cytotoxicity assays. As ExoT and ExoS are
141 known to specifically induce cell shrinkage and disruption of the actin cytoskeleton, we
142 quantified cell rounding of infected cells over time[10]. For this purpose, NCI-H292 cells were
143 incubated prior to infection with a red fluorescent probe that labeled the cell cytoplasm, and
144 fluorescence representing the total surface area was monitored using automated time-lapse
145 microscopy. As the ExoY variants were co-injected with a single T3SS effector, either ExoT or
146 ExoS, the cytotoxicity observed could be directly linked to these effectors and potential
147 synergistic effects with the co-injected ExoY variant. Indeed, a strain deleted for ExoS and ExoT
148 but injecting only ExoY did not induce rapid cell retraction as compared to a strain injecting
149 both ExoT and ExoY (Figures 2A and 2B).

150 With PAO1FΔS strains co-injecting ExoT with WT ExoY or ExoY^{mut2}, we observed similar
151 kinetic profiles of cell rounding (Figures 2C and 2D). In contrast, ExoT-induced cell rounding
152 was faster when the toxin was co-injected with the ExoY^{mut0}, ExoY^{mut1} or ExoY^{mut3}, variants
153 with deficient or significantly diminished cGMP-synthetizing activity (Figure 1J). Hence, strains
154 expressing an ExoY variant deficient in cGMP production exhibited exacerbated ExoT-
155 mediated cytotoxicity. Notably, this effect was not due to increased injection of ExoT, as
156 comparable protein levels were detected in infected cells (Figures S3A and S3B).

157 Similar experiments were carried out with the PAO1FΔT derivatives to analyze
158 potential synergistic effects between ExoS and the ExoY variants. Interestingly, retraction
159 curves for all strains examined were similar, indicating that ExoY did not alter ExoS-mediated
160 cell rounding (Figures 2E and 2F). However, the PAO1FΔT derived strains failed to trigger a
161 significant cGMP increase in infected cells as compared to the PAO1FΔS strains co-injecting

162 ExoT with WT ExoY or ExoY^{mut2} (Figures 2G and S3C). We considered two hypotheses to explain
163 the absence of detectable cGMP (the main cNMP produced by WT ExoY) levels in cells infected
164 with PAO1FΔT strains: i) Feedback inhibition of T3SS effectors injection by ExoS[45,46] that could
165 have prevented ExoY from being efficiently injected, or ii) ExoS interference with the
166 activation of ExoY by F-actin. Both scenarios would indeed result in a lack of cNMP
167 accumulation in infected cells. Western blot (WB) analysis showed that both ExoS and ExoY
168 were well secreted and injected into cells by the different strains (Figures S3A and S3B), ruling
169 out the first hypothesis. ExoS therefore appears to interfere with the activity/activation of
170 ExoY, which therefore cannot produce cNMPs and thus cannot influence ExoS-induced
171 cytotoxicity. This point is further examined below.

172 **ExoY-synthesized cGMP specifically alters the downstream effects of ExoT ADPRT activity**

173 ExoT and ExoS are bifunctional toxins with an N-terminal GTPase-activating protein (GAP)
174 domain and a C-terminal ADP-ribosyltransferase (ADPRT) domain, both of which contribute to
175 cell shrinkage. However, the domain responsible for cell rounding varies across cell types[32,47–
176 51]. To elucidate how ExoT and ExoS mediate cell rounding in our cell model, we investigated
177 the contributions of their GAP and ADPRT activities. Point mutations were introduced into the
178 genomes of PAO1FΔS or PAO1FΔT strains to selectively inactivate each activity[48–50,52–58]
179 (Figure 3A). Cell rounding was then evaluated in cells infected with the mutant strains. Our
180 results showed that the ADPRT activity of both toxins primarily drives cell retraction in NCI-
181 H292 cells (Figures 3B, 3C, S4A and S4B). The data further indicated that the GAP activity of
182 ExoT partly counteracted the cell rounding induced by the ADPRT domain of ExoT, as the total
183 cell surface area was significantly lower after 8 hours of infection with ExoT^{GAP-} mutant as
184 compared to WT ExoT. Given that ExoY-derived cGMP attenuates ExoT cytotoxicity, we
185 therefore hypothesized that in NCI-H292 cells, ExoY-synthesized cGMP specifically interferes
186 with ExoT ADPRT activity and/or its downstream effects, thereby protecting cells from
187 rounding.

188 To test this hypothesis, we generated a chimeric ExoT variant by replacing the ExoT
189 ADPRT domain with that of ExoS (Figure 3D). The variant was introduced into PAO1FΔS strains
190 via allelic exchange, and cytotoxicity assays were performed on cells infected with *P.*
191 *aeruginosa* strains injecting either WT or chimeric ExoT variants. As shown above, the ExoT-
192 induced cell rounding was dampened by the co-injection of the WT ExoY as compared to that

193 observed upon co-injection of the ExoY variants unable to produce cGMP (ExoY^{mut0} and
194 ExoY^{mut1}) (Figure 3E and 3F). In contrast, the cell retraction induced by the chimeric
195 ExoT^{ADPRT_ExoS} was not affected by the ability of co-injected ExoY variants to generate cGMP.
196 Furthermore, the cell retraction caused by the chimeric ExoT$^{ADPRT\text{-}ExoS}$ was comparable to that
197 induced by ExoS, confirming that the chimera is functional in cells. These results demonstrate
198 that cGMP synthesized by ExoY specifically interferes with the signaling pathway targeted by
199 ExoT's ADPRT domain, thereby attenuating ExoT's disruptive impact on the host cell
200 cytoskeleton. These results also highlight that the ExoS ADPRT activity is either insensitive to
201 ExoY cGMP production or, more likely, that ExoS ADPRT activity counteracts ExoY activity as
202 illustrated by the absence of detectable cGMP (Figures 2G and S3C).

203 **In NCI-H292 cells, ExoS ADPRT activity restricts ExoY activation**

204 We infected the luminescent cGMP reporter cell line, representing intracellular cGMP
205 production, with PAO1FΔS or PAO1FΔT strains to test the hypothesis that, compared with
206 ExoT, ExoS activity interferes with ExoY activation and thus with its production of cGMP.
207 Luminescence intensities after infection of the reporter cell line with recombinant PAO1FΔS
208 strains co-injecting ExoY with ExoT or ExoT variants were all similar to those obtained when
209 ExoY was injected alone, indicating that, as expected, ExoT activities do not prevent ExoY from
210 being active (Figure 3G). In contrast, co-injection of active ExoS toxin with ExoY decreased the
211 intensity of luminescence corresponding to cGMP production compared with injection of ExoY
212 alone (Figure 3H). Only co-injection of an ExoS variant with inactive ADPRT activity completely
213 restored cGMP production by ExoY in NCI-H292 cells, validating the above proposition that
214 ExoS ADPRT activity impedes ExoY activity. The lack of ExoY activity could result from a local
215 inhibition of actin polymerization by the ADPRT activity of ExoS, thus disrupting the activation
216 of ExoY. As a result, compared to ExoT, ExoS activity prevents the toxin from a possible
217 feedback inhibition by ExoY-synthesized cGMP.

218 **CrkII is the downstream target of ExoT's ADPRT activity modulated by ExoY-induced cGMP**

219 The GAP domains of ExoS and ExoT target the same Rho family GTPases, including Rho, Rac1
220 and Cdc42[47,49,52,59], while their ADPRT domains target distinct cellular proteins. ExoS ADP-
221 ribosylates various proteins, such as Ras, Rac1 and the ERM family[48,60–65], whereas ExoT ADP-
222 ribosylates Crk family proteins and actin[66–69]. Since cGMP production by ExoY only altered

223 ExoT's ADPRT activity, we reasoned that this effect might depend primarily on the eukaryotic
224 targets of ExoT's ADPRT, namely the Crk proteins.

225 We therefore evaluated the possibility that Crk family proteins are involved in the
226 cGMP-antagonized ExoT cytotoxicity, by generating Crk$^{-/-}$ NCI-H292 cells using CRISPR-Cas9
227 technology. For this purpose, a gRNA was designed to specifically target the *crk* gene and not
228 the *crkL* gene (Figure S5A). The *crk* gene encodes two spliced products, CrkI and CrkII, which
229 differ in size. CrkII has an additional SH3 domain at its C-terminus, resulting in a 40 kDa protein,
230 whereas CrkI is a 28 kDa protein (Figure 4A). The *crkL* gene encodes a paralogous Crk-like
231 protein (CrkL) that shares high sequence homology with CrkII. All three proteins are
232 considered adaptor proteins and play an essential role in integrating signals from a wide
233 variety of cellular processes[70,71]. However, since ExoT ADP-ribosylation has been described to
234 modify CrkI/II proteins and not CrkL, we focused our analysis on CrkI/II proteins.

235 A clonal population was selected, in which four bases were deleted from the beginning
236 of the coding sequence of the *crk* alleles, theoretically ablating the expression of WT CrkI/II
237 proteins (Figure S5A). Both CrkI and CrkII production were indeed knocked-out in deficient
238 cells compared to WT cells (Figure S5B). Low-intensity bands of the same size as CrkI and CrkII
239 were nevertheless detected in deficient cells. This suggests that the obtained clones were not
240 fully depleted of CrkI/CrkII, possibly because complete depletion could be detrimental to cell
241 physiology. WT and Crk-deficient cells were then infected with PAO1FΔS strains and cell
242 rounding was recorded as previously described. In contrast to WT cells, Crk$^{-/-}$ cells showed a
243 reduced ExoT-induced cell rounding, represented by an increase in the area under the curve
244 (AUC), with no significant difference between strains regardless of the co-injected ExoY
245 effector variant (Figure 4B and S6A-S6D). These data indicate that CrkI and/or CrkII are the
246 downstream targets of the ExoT/ADPRT activity blunted by ExoY-synthesized cGMP. To
247 identify the Crk isoform involved, Crk-deficient cells were complemented with a lentiviral
248 plasmid encoding either CrkI or CrkII. Rescuing CrkII expression in Crk deficient cells resulted
249 in infection profiles with PAO1FΔS strains similar to those observed in wild-type cells, whereas
250 CrkI expression did not restore similar profiles (Figure 4B, 4C and S6E-S6H). Crk$^{-/-}$::CrkII cells
251 were indeed as sensitive as WT cells to cGMP-dependent ExoT cytotoxicity. These results
252 confirmed that CrkII is the main target of the cytotoxicity of ExoT modulated by ExoY during
253 the infection of the cells.

254 **ExoY-synthesized cGMP dampens CrkII dephosphorylation induced by ExoT's ADPRT activity**

255 CrkII is a part of focal adhesion (FA) complexes composed of kinases (Src and FAK), docking
256 molecules (p130cas, paxillin) and downstream proteins such as DOCK180 and C3G. Upon
257 stimulation, CrkII is tyrosine-phosphorylated at Y221 by activated Abelson's tyrosine-protein
258 kinase (Abl)[72–75], and translocated to the membrane[73,76–78] where the adaptor protein CrkII is
259 dephosphorylated to interact with tyrosine-phosphorylated p130cas[77,79–85] and other
260 partners, leading to actin cytoskeleton reorganization, cell migration and cell spreading[86].
261 However, Crk signal transduction pathways are disrupted after injection of ExoT by *P.*
262 *aeruginosa*. Abl/CrkII interaction and CrkII phosphorylation[73,87] are inhibited by ExoT through
263 ADP-ribosylation of cytoplasmic CrkII at Arg20[66], thus preventing CrkII membrane localization.
264 In addition, CrkII interaction with upstream signaling molecules such as activated p130cas is
265 also inhibited by ExoT ADP-ribosylation[69]. Therefore, ExoT's ADPRT activity induces loss of cell
266 adhesion and cell-matrix interaction, leading to cell rounding and eventually to a programmed
267 apoptotic cell death called anoikis[69,88,89].

268 We therefore explored whether the ExoY-synthesized cGMP could limit the ExoT-
269 induced CrkII dephosphorylation at Y221. CrkI, CrkII and phospho-CrkII (at Y221) levels were
270 analyzed by WB after infection of cells with the different PAO1FΔS strains (Figure 4D). CrkI and
271 CrkII levels remained constant after four hours of infection, while phospho-CrkII levels were
272 drastically reduced in infected cells as compared to the uninfected condition but were similar
273 regardless of the PAO1FΔS strain used for infection. Furthermore, the level of phospho-CrkII
274 was similar between the uninfected condition and the conditions in which cells were infected
275 for four hours with the strains PAO1FΔST (ExoY injection only) and PAO1FΔSTY (injecting none
276 of the T3SS effectors) (Figure 4D). These results indicate that: (i) ExoT cytotoxicity leads to
277 CrkII dephosphorylation, as previously described[73,87], and (ii) injection of active WT ExoY alone
278 does not alter phospho-CrkII level *per se*. It should be noted that in NCI-H292 cells, prior to
279 infection, CrkII is highly phosphorylated. Infection was therefore repeated at different times
280 to follow kinetics of CrkII dephosphorylation by ExoT activity in order to visualize potential
281 differences between the strains related to the distinct NC activities of the injected ExoY
282 variants. As shown in Figure 4E, phospho-CrkII levels were not altered over time when cells
283 were infected with the PAO1FΔST strain, injecting only active ExoY, demonstrating that cGMP
284 production by ExoY is not directly involved in CrkII phosphorylation nor in altering phospho-

285 CrkII levels. However, as expected, CrkII is dephosphorylated over time due to the ExoT activity
286 co-injected with ExoY. Interestingly, when ExoT is co-injected with ExoY variants defective in
287 cGMP production (ExoY^{mut0}, ExoY^{mut1} or ExoY^{mut3}), the rate of CrkII dephosphorylation by ExoT
288 activity is increased, particularly after 2h of infection (Figures 4E and 4F). These data
289 demonstrated that the cGMP produced by ExoY attenuated the ExoT-dependent CrkII
290 dephosphorylation at Y221 in infected NCI-H292 cells, thereby decreasing ExoT's ADPRT-
291 mediated cytotoxicity (Figures 2C and 2D).

292 To confirm that cGMP is directly involved in the modulation of the ExoT-induced CrkII
293 dephosphorylation, the infection medium was supplemented with compounds that stimulate
294 cGMP production in cells and phospho-CrkII levels were analyzed by WB during infection.
295 Spermine NONOate is indeed a nitric oxide donor that activates soluble guanylate cyclases
296 (GCs) and thus intracellular cGMP production[90] while 8-Br-cGMP is a cell-permeable cGMP
297 analog that is more resistant to hydrolysis by phosphodiesterases than cGMP. When infected
298 with the strain co-injecting ExoT with ExoY^{mut0} (unable to produce all cNMPs), the addition of
299 either compound limits CrkII dephosphorylation over time by ExoT activity, compared with the
300 condition without these compounds (Figure 4G and 4H).

301 These results, together with the above data, highlight the complex interaction
302 between ExoY and ExoT effectors in infected cells as illustrated in Figure 5. Whereas CrkII is
303 dephosphorylated as a downstream effect of ADPRT activity of ExoT, leading to cell rounding,
304 cGMP produced by ExoY delays this dephosphorylation and thus limits the ExoT-induced cell
305 rounding.

306 **Inhibition of ExoT cytotoxicity by ExoY depends on cell model**

307 To reinforce and generalize our discovery on the interaction between ExoT and ExoY, we
308 examined their effects on other epithelial cell lines commonly used in studies of *P. aeruginosa*
309 infection, HeLa cells[49,51] and A549[13,18,46] alveolar epithelial cells.

310 Co-injection of ExoT with ExoY^{mut0} or ExoY^{mut1} resulted in an increase in ExoT-induced
311 cell retraction in HeLa cells compared to ExoY WT (Figures 6A and 6B), similarly to what was
312 observed with NCI-H292 cells (Figures 2C and 2D), although the overall effect was less
313 pronounced. As similar levels of ExoT were injected by these strains (Figure 6C) we concluded
314 that, as in NCI-H292 cells, the guanylate cyclase negative variants ExoY^{mut0} and ExoY^{mut1} could
315 not inhibit ExoT cytotoxicity. However, in contrast to NCI-H292 cells where only the ADPRT

316 activity of ExoT is involved in cell retraction, we found that in HeLa cells, the GAP activity of
317 ExoT also plays an important role in cell retraction (Figure 6D). So, since ExoY-synthesized
318 cGMP only dampens ExoT's ADPRT activity, its effect on ExoT cytotoxicity is weaker in HeLa
319 cells, in contrast to NCI-H292 cells, where ExoT cytotoxicity is entirely ADPRT-dependent.
320 Another interesting observation is that the HeLa cell rounding was drastically increased upon
321 infection with strains co-injecting ExoT with ExoY^{mut2} or ExoY^{mut3} (Figures 6A and 6B). This
322 increase in strain virulence is likely due to the significant over-injection (up to three-fold) of
323 ExoT into cells when co-injected with these two ExoY mutants, as revealed by WB (Figure 6C).
324 Whether this hypertranslocation is linked to the higher AC activity of ExoY^{mut2} and ExoY^{mut3},
325 and the putative mechanisms involved, remain to be clarified.

326 Similar *P. aeruginosa* infection experiments were carried out on A549 alveolar
327 epithelial cells. In contrast to NCI-H292 and HeLa cells, the co-injection of ExoY did not
328 counteract ExoT cytotoxicity in A549 cells, as the ExoT-induced cell retraction curve was
329 indistinguishable from those obtained with the defective GC variants, ExoY^{mut0} and ExoY^{mut1}
330 (Figures 7A and 7B). WB confirmed that similar levels of ExoT were injected by all three strains
331 (Figure 7C). However, only very low levels of cGMP (and cAMP) were measured in A549 cells
332 infected with the PAO1FΔS strain, indicating a severe defect in ExoY activation in these cells
333 at variance with what was seen in NCI-H292 cells (Figure 7D). Additionally, the A549 cell
334 rounding seems to depend solely on the GAP activity of ExoT and not on its ADPRT activity, in
335 contrast to NCI-H292 cells (Figure 7E). Furthermore, given that CrkII was the key component
336 mediating the synergy between ExoT and ExoY effectors in NCI-H292 cells, we examined CrkI
337 and CrkII expression levels in A549 cells by WB. While CrkI levels were similar between cell
338 lines (Figure 7F), CrkII levels were extremely low in A549 cells, comparable to those found in
339 Crk-deficient NCI-H292 cells (Figure S5B). This lack of CrkII expression likely explains why ExoT-
340 induced cell rounding in A549 cells is entirely driven by the GAP activity of ExoT rather than
341 its ADPRT activity. Moreover, as with HeLa cells, ExoT-induced cell rounding was markedly
342 enhanced when A549 cells were infected with strains co-injecting ExoT with ExoY^{mut2} or
343 ExoY^{mut3} (Figures 7A and 7B). This increase in ExoT cytotoxicity was again likely due to the
344 higher amounts of ExoT injected into A549 cells by these two PAO1FΔS strain derivatives
345 (Figure 7C).

346 Overall, the comparison of *P. aeruginosa* infection outcome in the three different cell
347 lines showed that ExoY cNMP production affects ExoT cytotoxicity in a complex, cell-

348 dependent manner, influenced by ExoT's activity involved in cell rounding and by CrkII
349 expression. The downstream effects of ExoT's ADPRT activity are tempered by ExoY's
350 production of cGMP, while the downstream effects of ExoT's GAP activity are unaffected
351 possibly because it may prevent ExoY activation.

352 **Discussion:**

353 ExoY is a member of the bacterial nucleotidyl cyclase (NC) family, alongside CyaA from
354 *Bordetella pertussis* and Edema Factor (EF) from *Bacillus anthracis*, which manipulate host
355 cNMP signaling pathways to enhance pathogen survival and proliferation. However, instead
356 of producing supraphysiological levels of cAMP like CyaA and EF, ExoY generates large
357 amounts of cGMP. To our knowledge, no specific function has been ascribed to the cGMP
358 produced by ExoY during infection. Our results demonstrate that in NCI-H292 cells, cGMP
359 production by ExoY attenuates the cytotoxicity of ExoT, the only T3SS effector conserved in all
360 T3SS-expressing *P. aeruginosa* strains. When ExoY variants defective in cGMP production were
361 co-injected with ExoT, ExoT-induced cell retraction was exacerbated. On the contrary, ExoS
362 cytotoxicity, was not inhibited by ExoY in this cell line. The reduced cGMP generation observed
363 under these conditions likely explains the absence of an ExoY-mediated effect. We
364 hypothesize that ExoS, via its ADPRT activity, can locally disrupt the actin polymerization
365 thereby suppressing the F-actin-dependent ExoY activation and consequently cGMP synthesis.
366 We therefore further examined how ExoY modulates ExoT cytotoxicity in NCI-H292 cells. We
367 focused on the ADPRT domain of ExoT and its targets, the Crk family proteins, as ExoT-
368 mediated cell retraction is driven by ExoT's ADPRT activity. In the NCI-H292 cell model, we
369 found that when ExoY and ExoT are co-injected, ExoY-derived cGMP limits the ExoT-mediated
370 dephosphorylation of CrkII at Y221, which occurs as a result of ADP-ribosylation. As a
371 consequence, by limiting CrkII-Y221 dephosphorylation, ExoY-synthetized cGMP directly
372 attenuates ExoT cytotoxicity. Conversely, ExoY variants unable to produce cGMP had no effect
373 on ExoT-mediated CrkII dephosphorylation and thus on ExoT cytotoxicity, leading to rapid cell
374 retraction by disruption of focal adhesion sites.

375 The molecular mechanisms that link the ADP-ribosylation of CrkII by ExoT and its Y221
376 dephosphorylation remains to be precisely elucidated, as well as how the cGMP produced by
377 ExoY can interfere with this process. It has been described that (i) CrkII is specifically
378 dephosphorylated by PTP1B[85] and that (ii) PTP1B phosphatase activity can be indirectly
379 regulated by cGMP. Indeed, PTP1B is regulated by EGFR[91,92] whose activation is controlled by
380 cGMP-dependent protein kinases (PKGI and PKGII)[93–96]. Activation of these kinases by cGMP
381 may thus inhibit EGFR activation and, consequently, reduce PTP1B activity. We therefore
382 propose that during infection of NCI-H292 cells by *P. aeruginosa*, two mechanisms occur:

383 Firstly the ADPRT activity of ExoT limits the production of phosphorylated CrkII by preventing
384 the interaction between CrkII and Abl[73,87], and secondly, the phosphatase activity of PTP1B
385 further reduces the level of previously phosphorylated CrkII. Together, these mechanisms lead
386 to rapid dephosphorylation of CrkII at Y221 and consequently induce cell rounding through
387 loss of cell adhesion and cell-matrix interaction. However, high cGMP levels generated by
388 activated ExoY could inhibit PTP1B phosphatase activity, via the activation of cGMP-
389 dependent protein kinases and the mechanism suggested above, reducing CrkII
390 dephosphorylation by PTP1B and thus limiting the downstream effects of ExoT's ADPRT
391 activity.

392 The antagonistic effect of ExoY-derived cGMP on the cytotoxicity of ExoT is however
393 complex and depends on the type of host cells infected and on the predominant mechanism
394 used by ExoT to induce its toxic effects (GAP vs ADPRT). For instance, in A549 cells, where the
395 cytotoxicity of ExoT relies on its GAP activity, we found that the injected ExoY did not produce
396 cGMP. Likely, as with the ADPRT activity of ExoS in NCI-H292 cells, the GAP activity of ExoT in
397 A549 cells may have disrupted the ExoY's activator and consequently cGMP production. As a
398 result, ExoY had no protective effect against ExoT cytotoxicity in these cells. In HeLa cells, as
399 the cytotoxicity of ExoT depends on both its GAP and ADPRT activities, ExoY has only a limited
400 protective effect. The conditions determining whether ExoT cytotoxicity depends primarily on
401 its GAP or ADPRT activity remain to be elucidated. One determinant could be the expression
402 of CrkII in the cells. When CrkII is expressed, ExoT can induce cell retraction by either or both
403 of its activities, as seen in the infection of NCI-H292 and HeLa cells. Conversely, when CrkII is
404 not expressed, ExoT can induce cell rounding solely by its GAP activity, as seen in the infection
405 of A549 cells.

406 We previously showed that the presence of a T3SS effector gene does not guarantee
407 that it will be injected and activated in the host target cells[30]. Our present study now
408 demonstrates that the type of host cells targeted, the combination of T3SS effectors injected
409 and their mechanism used to induce cytotoxicity can also affect effector activation. Indeed,
410 ExoY is inactive when co-injected with ExoS and also potentially when the cytotoxicity of ExoT
411 depended specifically on its GAP activity. Our findings reveal that ExoS and ExoT not only exert
412 their own cytotoxic effects, but also play a critical role in ExoY activation and, consequently,
413 in their own feedback regulation by ExoY-synthesized cGMP.

414 The study of interplay between multiple effectors is challenging, particularly when two
415 effectors induce similar cytotoxic effects. In this case, both ExoT and ExoS trigger cell
416 retraction. To address this, we focused on examining two effectors at a time: ExoY with ExoT
417 and ExoY with ExoS. We believe that what happens when the three effectors are delivered
418 together may involve even more complex regulatory mechanisms than those described here.
419 The interaction between co-delivered effectors could represent a dynamic interplay, with
420 outcomes influenced by effector ratios, the specific cell line, or the stage of infection.
421 Furthermore, the overall effect of these interactions may be modulated by the infection
422 environment, including host cell responses, which can ultimately alter the final outcome.
423 To conclude, this work reveals a critical role for ExoY-synthetized cGMP in modulating
424 T3SS effector cytotoxicity, particularly that of ExoT, and highlights how *P. aeruginosa* might
425 fine-tune its virulence to potentially optimize host colonization or establish and/or maintain
426 chronic host infection. The ability of ExoY to modulate ExoT cytotoxicity in a context
427 dependent manner may explain the widespread presence of ExoY among *P. aeruginosa*
428 strains. Indeed, *P. aeruginosa* may benefit from a regulatory factor such as ExoY, which can
429 modulate the bacterium's pathogenicity linked to ExoT cytotoxicity. The cNMPs produced by
430 ExoY could adjust *P. aeruginosa* infection strategies to the cellular context, expanding the
431 repertoire of host cell manipulation by the bacterium throughout the progression of infection.
432 Additional unexplored effects of ExoY-produced cNMPs likely exist and remain to be
433 discovered.

434 **Materials & Methods**

435 **Antibodies and reagents**

436 The mouse recombinant monoclonal Crk p38 antibody, targeting CrkI and CrkII was purchased
437 from Abcam (#ab300630, dilution 1:1000). The rabbit Phospho-CrkII (Tyr221) antibody,
438 detecting endogenous levels of CrkII only when phosphorylated at Tyrosine 221, was
439 purchased from Cell Signaling Technology (#3491S, dilution 1:500). The mouse monoclonal
440 antibody against β-actin was from Sigma Aldrich (#A2228, dilution 1:10000). The HRP-labeled
441 detection antibody, IgG Detector Solution V2, was from the TAKARA kit named Western BLoT
442 Rapid Detect v2.0 (# T7122A) and was used at a dilution of 1:3000. Rabbit polyclonal
443 antibodies specific to ExoS and ExoT were obtained from Arne Rietsch and used at a dilution
444 of 1:5000 (Case Western Reserve University School of Medicine). The specific antiserum for
445 ExoY was obtained from Covalab and created by injecting rabbits with recombinant, truncated
446 ExoY (aa26-223) with a His-tag at its C-terminus. This ExoY antibody was used at a dilution of
447 1:2000. The Cytotrace Red CMTPX was purchased from Cayman (#20698) and diluted to 1mM
448 with DMSO. Puromycin (#UP9200-A) and geneticin (#10131027) antibiotics were purchased
449 from EUROMEDEX and Gibco, respectively. The Polybrene was from MERCK MILLIPORE (#TR-
450 1003). The cOmplete EDTA-free protease inhibitor cocktail was from Roche (#11873580001)
451 and the Bradford reagent was from BioRad (Protein Assay Dye Reagent Concentrate,
452 #5000006). Spermine NONOate was purchased from ENZO LIFE SCIENCES (#ALX-430-013-
453 M005) and diluted in water to obtain a 50 mM stock solution. 8-Bromoguanosine 3',5'-cyclic
454 monophosphate (8-Br-cGMP) was purchased from SIGMA ALDRICH CHIMIE (#B1381-10MG)
455 and diluted in water to obtain a 100 mM stock solution.

456 **Bacterial strains and growth conditions**

457 The bacterial strains and plasmids used in this study are listed in Supplementary Table 1.
458 Bacterial strains were grown in Luria-Bertani (LB) medium at 37 °C with shaking (180 rpm).
459 Antibiotics were added at the following concentrations: Ampicillin at 100 µg mL−1,
460 gentamycin at 15 or 30 µg mL−1 for *E. coli* and *P. aeruginosa*, respectively. For infection assays,
461 overnight cultures were diluted to optical density (OD_{600}) of 0.1 and grown under agitation to
462 reach OD_{600} of 1.

463 **Eukaryotic cell lines and growth conditions**

464 The human embryonic kidney (HEK) 293 T (ATCC CRL-3216), A549 (ATCC CCL-185) and HeLa
465 (ATCC CCL-2) cells were cultured in Dulbecco's modified Eagle's medium (DMEM)
466 supplemented with 10% fetal bovine serum (FBS). The NCI-H292 cells and their derivatives
467 were cultured in RPMI 1640 medium with GlutaMAX™ supplemented with 10% FBS. Cells
468 transfected with pLVX-IRES-neo vector encoding cAMP or cGMP GloSensor or encoding CrkI
469 or CrkII, were maintained by addition of 200 µg mL−1 Geneticin to the supplemented medium.
470 Cells were grown at 37 °C with 5% CO2 and routinely passaged.

471 **Plasmid construction**

472 Primers used for PCR amplification, mutations or sequencing are listed in Supplementary Table
473 2.

474 pB26 expressing ExoY$^{K81M-K88I}$-FH (ExoY^{mut0}-FH) was created by exchanging the PaeI/Bsp119I
475 fragment from pUM460[14] by that of p1682[22].

476 pUM717 expressing ExoY$^{N264V-F289V-S292G-D293A}$-FH (ExoY^{mut1}-FH), was created by exchanging the
477 SphI/NdeI fragment from pUM460 by that of pUM700 (see below).

478 For pUM721, site-directed mutagenesis to introduce the mutation specifying the F83L
479 exchange into *exoY* was performed by PCR amplification with primers VD5-F83L_F and VD5-
480 F83L_R on template pUM460. Nonmutated plasmid (template) was digested by FastDigest
481 DpnI (ThermoFisher, #FD1703) and the reaction mixture was transformed into DH5α. Plasmid
482 DNA of a verified clone was digested with Bsp119I and SphI to subclone the fragment coding
483 for the F83L mutation into an unmodified pUM460 vector digested with Bsp119I and SphI.
484 Subcloning was performed to exclude potential PCR-introduced mutations in the vector
485 sequence.

486 For pUM727 (expressing ExoY^{mut2}-FH), primers VD11-S292G_F and VD11-S292G_R were used
487 to introduce the mutation coding for the S292G exchange into pUM460 as described above.
488 The Bsp119I/NdeI fragment specifying the S292G mutation, was then inserted into the
489 pUM721, already containing the F83L mutation.

490 For pUM733 (expressing ExoY^{mut3}-FH), the E258D mutation was added to pUM727 as
491 described above, using the oligonucleotide primers VD13-E258D_F and VD13-E258D_R. The
492 Bsp119I/NdeI fragment, containing the S292G and E258D mutations, was then inserted into
493 the pUM721.

494 The pVR2 expressing AcGFP under the $P_{TRE3G-BI}$ promoter was created by inserting the
495 BamHI/Not1 fragment of pAcGFP-N1, coding for AcGFP, into MCS1 of pTRE3G-BI. Next, the
496 *exoY* gene of pUM445[14] was amplified by PCR with primers UM245 and UM374 and cloned
497 into EcoRI/MluI-digested MCS2 of pVR2, yielding pUM542.
498 The expression plasmid pUM546 was constructed by replacing the SmaI/RsrII fragment of
499 p1682[22] (containing the K81M and K88I mutations in ExoY, $ExoY^{mut0}$) into pUM542.
500 The plasmid pUM700 encoding ExoY with the N264V, F289V, S292G and D293A mutations
501 ($ExoY^{mut1}$) was created in two steps. First, site-directed mutagenesis was used on pUM460, as
502 described previously, with primers VD-N264V_F and VD-N264V_R to introduce the N264V
503 mutation. This was followed by another site-directed mutagenesis using primers VD-F289V-
504 S292G-D293A_F and VD-F289V-S292G-D293A_R to introduce the F289V, S292G and D293A
505 mutations. After digestion of the non-mutated plasmid with DpnI, the sequence verified
506 mutated plasmid was digested with Bsp119I and NcoI and the extracted fragment was cloned
507 into pUM542 digested with the same restriction enzymes to replace the WT fragment of the
508 *exoY* gene.
509 Transfection plasmid pUM731, encoding $exoY^{F83L-S292G}$ ($exoY^{mut2}$), was created by exchanging
510 the NcoI/ SphI fragment from pUM542 by that of pUM727.
511 Similarly, pUM734, encoding $exoY^{F83L-E258D-S292G}$ ($exoY^{mut3}$), was created by exchanging the
512 NcoI/ SphI fragment from pUM542 by that of pUM733.
513 pUM517 was created by PCR-amplification of pUM445[14] with UM345 and UM246 and cloning
514 of the fragment into NheI/XhoI-digested pAcGFP-N1.
515 The construction of pUM549, to introduce by allelic exchange the K81M and K88I
516 mutations ($ExoY^{mut0}$) into the *exoY* of PAO1F strains as well as the region coding for a C-
517 terminal Flag-His tag, was carried out in several steps. First, an intermediate plasmid named
518 pB93Gm was created, containing the *exoY* sequence including the genomic sequences located
519 upstream and downstream of the gene. To this end, a PCR reaction amplifying the genomic
520 sequence upstream of *exoY* was performed on PAO1 genomic DNA (gDNA) using primers #124
521 and #125 and incorporated into plasmid pEX18Gm as HindIII/PstI fragment. Subsequently, a
522 fragment containing the genomic sequence downstream of *exoY* was PCR-amplified from
523 gDNA of PAO1 using primers #126 and #127 and introduced into this plasmid as XbaI/EcoRI
524 fragment. A fragment coding for *exoY* and a C-terminal Flag-His tag was then PCR amplified
525 from pUM460 using primers #128 and #129 and inserted as PstI/XbaI fragment into the

526 previous plasmid yielding pB93Gm. Finally, the sequence coding for the K81M and K88I
527 mutations (mut0) was introduced into pB93Gm by replacing the BamHI/SphI fragment with
528 that of p1682[22] to yield pUM549.
529 pUM707 was created to introduce *exoY* alleles coding for variants ExoY^{mut1}, ExoY^{mut2} and
530 ExoY^{mut3} into PAO1F by allelic exchange. To construct pUM707, a 2032-bp fragment was PCR
531 amplified from chromosomal DNA of PAO1FΔS using primers PAO1-Up_F and PAO1-Down_R
532 and inserted into pEX18Gm between the EcoRI and HindIII sites.
533 NcoI/SphI fragments specifying the mutations in ExoY^{mut1}, ExoY^{mut2} and ExoY^{mut3} were then
534 isolated from plasmids pUM700, pUM727 and pUM734 to replace the corresponding
535 fragment in pUM707 yielding pUM712, 728 and 736 respectively.
536 For the construction of the allelic exchange plasmid used to inactivate the Rho-GAP
537 domain of ExoS (R146K mutation), two PCR fragments were amplified from PAO1F
538 chromosomal DNA: PCR1 was performed with primers ExoSR146K-Up_F and ExoSR146K-
539 Up_R, and PCR2 was performed with primers ExoSR146K-Down_F and ExoSR146K-Down_R.
540 Next, a splicing by overlap extension PCR (SOE-PCR) was performed to combine the two PCR
541 fragments using equimolar amounts of PCR1 and PCR2 and the external primers (ExoSR146K-
542 Up_F and ExoSR146K-Down_R). The SOE-PCR fragment obtained was digested with EcoRI and
543 HindIII to replace the EcoRI/HindIII fragment of pUM707, yielding pUM737.
544 To generate the plasmid for inactivation of the ADPRT domain of ExoS (E379D and E381D
545 mutations), the same protocol was applied but with primers ExoSE379/381D-Up_F and
546 ExoSE379/381D-Up_R for the PCR1, and the primers ExoSE379/381D-Down_F and
547 ExoSE379/381D-Down_R for the PCR2, resulting in pUM738.
548 The mutation coding for R149K in *exoT* inactivating its Rho-GAP was introduced into the allelic
549 exchange vector using primer pairs ExoTR149K-Up_F/ExoTR149K-Up_R and ExoTR149K-
550 Down_F/ExoTR149K-Down_R for SOE-PCR and replacing the EcoRI/HindIII fragment in
551 pUM707, yielding pUM739.
552 The mutations coding for E383D and E385D in *exoT* inactivating its ADPRT domain were
553 introduced into the allelic exchange vector using primer pairs ExoTE383/385D-Up_F plus
554 ExoTE383/385D-Up_R and ExoTE383/385D-Down_F plus ExoTE383/385D-Down_R for SOE-
555 PCR and inserted as BamHI/HindIII fragment into pEX18Gm, yielding pUM740.
556 pUM752 was created to replace the ADPRT domain of ExoT by that of ExoS. To this end, three
557 PCR fragments were amplified from PAO1F chromosomal DNA: PCR1 was performed with

558 primers VD17_F and VD17_R (amplification of *exoS* ADPRT domain), PCR2 was performed with
559 primers VD18_F and VD18_R (amplification of *exoT* GAP domain) and PCR3 was performed
560 with primers VD19_F and VD19_R (amplification of the downstream *exoT* sequence). The
561 fusion of the three PCR fragments was performed in two steps. First equimolar amounts of
562 PCR fragments 1 and 2 were used for amplification with the outside primers VD18_F and
563 VD17_R (SOE-PCR1). Then, a second overlapping PCR (SOE-PCR2) was performed, containing
564 SOE-PCR1 and PCR3 at equimolar amounts and primers VD18_F and VD19_R. The obtained
565 fragment was digested with BamHI and HindIII and cloned into pEX18Gm.

566 **Purification of ExoY toxins**

567 ExoY-FH effectors encoded on pUM460, pB26, pUM717, pUM727 and pUM733 were
568 expressed from the λP_L promoter controlled by the temperature-sensitive cI repressor (cI857)
569 in *E. coli* BLR. 400 mL cultures in LB were started at an OD of 0.05 and incubated for 2h30 at
570 30°C before shifting the temperature to 37°C for 3h to express the proteins. Proteins were
571 purified from the insoluble protein fraction through their C-terminal His-tag using Ni-NTA
572 chromatography under denaturing conditions (in the presence of 8 M urea). Proteins were
573 renatured by dialysis into 20 mM Tris-HCl pH 9.0, 500 mM NaCl, 10% glycerol, 1 mM 1,4-
574 dithiothreitol (DTT) and 0.4 mM phenylmethylsulfonyl fluoride (PMSF).

575 **Quantification of cNMPs synthesis *in vitro* by ExoY proteins**

576 ExoY-catalyzed synthesis of cNMP was measured as described previously[14]. Reactions were
577 carried out for 10, 30 or 60 min at 30 °C in the presence of 3 µM of F-actin containing between
578 5 ng to 1 µg of ExoY proteins, and 2 mM NTP spiked with 0.1 µCi of [α-^{33}P] GTP, 0.1 µCi of [α-
579 ^{33}P] ATP, 0.1 µCi of [α-^{32}P] CTP or 0.1 µCi of [α-^{32}P] UTP. ^{33}P or ^{32}P were measured in a TriCarb
580 scintillation counter (Perkin Elmer). All reactions were performed in triplicates.

581 **Allelic exchange on *P. aeruginosa* strains**

582 Mutations on *exoS, exoT,* and *exoY* genes, on chromosomal DNA of PAO1F strains, were
583 incorporated using a two-step allelic exchange protocol as described before[97]. Sucrose
584 resistant allelic exchange mutants obtained after the second cross-over event were screened
585 using colony PCRs with Amplif-PAO1 primers for amplification of the fragment and Seq-PAO1
586 primers for sequencing, as specified in Supplementary Table 2. It should be noted that the
587 generation of GAP$^-$/ADPRT$^-$ double mutants on the *exoS* and *exoT* genes were carried out in

588 two steps. First, clones containing the GAP$^-$ mutation were selected, then pUM738 or pUM740
589 allelic exchange vectors were used on these clones to generate the inactivation of the second
590 domain. For the allelic exchange replacing the ADPRT domain of ExoT with that of ExoS, the
591 primers Amplif-PAO1-ExoS-ADPRT_F and Amplif_PAO1-ExoT_R were used to verify the
592 presence of the modified allele. Then PCR amplification from the selected colonies was
593 performed using Amplif-PAO1-ExoT_F and Amplif-PAO1-ExoT_R, followed by sequencing
594 using Seq-ExoT_F and Seq3-ExoS_F.

595 **cAMP and cGMP quantification in cells after infection by ELISA**

596 cAMP or cGMP were measured in cells using Direct cAMP/cGMP ELISA kits from Enzo Life
597 Sciences (#ADI-900-066A and #ADI-900-014, respectively). Cells were seeded at $1{,}5.10^5$ cells
598 per well in a 24-well plate and incubated for 2 days. After infection (see time indicated and
599 MOI used in figure legend), the cell medium was removed from each well and the cells were
600 washed with sterile PBS and frozen. Cells in each well were lysed with 54 µL of 0.1 M HCl
601 solution (supplied with the kit) and incubated for 30 min on ice, then scraped with a pipette
602 tip. The cell lysate was transferred to a 1.5 ml tube and centrifuged for 15 minutes at 12,000
603 rpm to remove cell debris. The protein concentration of each supernatant was then analyzed
604 by the Bradford assay and diluted to obtain the desired concentration specified by the
605 manufacturer. The non-acetylated protocol was followed for preparation of the cAMP and
606 cGMP standards as well as the samples. All samples were measured in duplicate. The yellow
607 color was read at 405nm.

608 **Lentiviral particles production**

609 Plasmids pGloSensor™-22F and pGloSensor™-40F were digested with NheI and XbaI and the
610 corresponding genes encoding Promega live-cell biosensors for cAMP and cGMP respectively,
611 were cloned into the pLVX-IRES-neo vector digested with SpeI and XbaI. Sequencing was
612 performed to select clones with inserts in the desired orientation. Next, lentiviral particles
613 containing the pLVX-neo-cAMP or pLVX-neo-cGMP plasmid were produced. For this, HEK 293T
614 cells were seeded in two 60 mm Petri dishes, each containing 3.10^6 cells and 5 mL of cell
615 medium and incubated for 24 h. The cells were then transfected using Lipofectamine 3000
616 transfection kit (Invitrogen, # L3000008) according to manufacturer's recommendations.
617 Briefly, 14 µL Lipofectamine 3000 and 12.8 µL P3000 Reagent were diluted separately in two
618 different tubes containing each 500 µL Opti-MEM (Gibco, #31985062). An appropriate mixture

619 of plasmids was added with the diluted P3000 Reagent in a 2:1 ratio of Transfection Reagent:
620 DNA complex. This mixture of plasmids was composed of the pLVX-neo-cAMP or pLVX-neo-
621 cGMP plasmid with the lentiviral packaging and envelope plasmids (psPAX2 and pMD2.G) at a
622 1:1:1 molar ratio (2.5 µg:2.5 µg:1.4 µg, respectively). The tubes were then mixed and
623 incubated 20 min at room temperature. The transfection mix was added to HEK293T cells in a
624 drop-wise manner and cells were incubated for 6 h. Following this incubation time, the
625 medium of each 60 mm Petri dish was replaced by 5 mL DMEM, containing 1,28% bovine
626 serum albumin (BSA) and 1x Pen/Strep. Transfected cells were incubated again for 72 h and
627 the lentiviruses containing media were finally harvested and centrifuged to pellet any
628 packaging cells that were collected during harvesting. Lentiviral particles were stored at −80
629 °C.

630 **Creation of stable cell lines with luminescent GloSensors**

631 NCI-H292 cells were seeded at 3.10^5 per well in a 6-well plate containing cell medium with
632 10% FBS and supplemented with 8 µg mL-1 polybrene to promote lentiviral infection. One mL
633 of lentiviral solution, containing the plasmid pLVX-neo-cAMP or pLVX-neo-cGMP was added
634 to the corresponding well. After 24 h incubation, the media was replaced with RPMI
635 containing 10% FBS, supplemented with 800 µg mL-1 Geneticin and cells were regularly
636 passaged until the uninfected cells were dead. The antibiotic concentration was then reduced
637 to 200 µg mL-1. Finally, clones were isolated by limiting dilution and clonal stable populations
638 were selected according to their luminescence emission upon intoxication with CyaA for
639 cAMP-GloSensor cells or transfection (see below with Xfect transfection kit) of plasmids
640 expressing ExoY (pUM517) or $ExoY^{K81M}$ (pUM518) for cGMP-GloSensor cells.

641 **Luminescence assay**

642 All plasmids for transfection were purified using the NucleoBond Xtra-Midi EF kit (Macherey-
643 Nagel, #740420).
644 Stable monoclonal cAMP-GloSensor and GMP-GloSensor cells were seeded at $1,5.10^4$ cells per
645 well in a 96-well plate (Corning, #3610), containing RPMI medium supplemented with 200 µg
646 mL-1 Geneticin. Cells were incubated for 2 days before co-transfection with the pEF1α plasmid
647 and the pUM542, pUM546, pUM700, pUM731 or pUM734 plasmids. The co-transfection was
648 performed using the Xfect™ Transfection Reagent (Takara, #631317) and according to
649 manufacturer's recommendations. Briefly, the media of each well was removed and replaced

650 by 100 µL per well of phenol red-free RPMI medium. Next, a mixture was prepared for each
651 condition containing 10 µL of Xfect reaction buffer, 0.15 µg of each plasmid and 0.09 µL of
652 Xfect polymer DNA (0.3 µL / µg DNA). The mixtures were incubated for 10 min at room
653 temperature to allow the nanoparticle complexes to form, and 10 µL of transfection solution
654 was added dropwise to the corresponding well. The plate was incubated at 37°C 5% CO_2 for 6
655 h before the cell medium was removed and replaced with RPMI supplemented with 200 µg
656 mL-1 Geneticin. The plate was incubated for 2 days at 37°C 5% CO_2 before removing the cell
657 medium and to replace it with RPMI containing 1 µg.mL-1 Doxycycline. After 3 h incubation,
658 the medium in each well was again removed and replaced with 100 µL / well of phenol red-
659 free RPMI containing 5% GloSensor cAMP reagent (Promega, #E1291). Luminescence was
660 monitored every 5 min for 4h at 24°C with an automated plate reader (Spark 10M by TECAN)
661 using an integration time of 1000 ms and the luminescence maximum (see representation on
662 Sup.Fig.2) was extracted.
663 For the infection experiments, 2.10^4 cGMP-GloSensor cells were seeded per well in a 96-well
664 plate for two days. The cell medium was removed, and the cells were infected at an MOI of
665 20 for 2 hours by adding 100 µL of resuspended bacteria in RPMI medium (Gibco, #32404014)
666 containing GlutaMAX (Gibco, #35050038). Then, 40 µL of resuspended GloSensor cAMP
667 reagent was added to each well to a final concentration of 3.6% and luminescence was
668 recorded every 3 min for 3.5 hours at 24°C.
669 For CyaA experiments, 2.10^4 cAMP-GloSensor cells were seeded per well in a 96-well plate for
670 two days. One hour before intoxication, the cell medium was removed and 90 µL of phenol
671 red-free RPMI medium containing GlutaMAX was added per well. This medium was also
672 supplemented with 2mM $CaCl_2$, 0,5% BSA and 5% GloSensor cAMP reagent. Cells were finally
673 intoxicated with 1nM final CyaA or $CyaA^{R12E}$ (mutant not translocated, negative control[98]) per
674 well and luminescence was recorded as previously described.

675 **Knock-out of *Crk* gene**

676 A pair of oligonucleotides corresponding to a gRNA targeting the *Crk* gene (Supplementary
677 Table 2) was phosphorylated and annealed before being cloned into the Esp3I-digested
678 pLentiCRISPRv2 vector. Then, as previously described, lentiviral particles containing the
679 recombinant plasmid pLentiCRISPR_Crk were created using the HEK293T cells and the psPAX2
680 and pMD2.G plasmids. NCI-H292 cells were afterwards infected with these lentiviruses using

681 1 mL of lentiviral particles in a well of a 6-well plate. Transfected cells were selected with 2
682 µg.mL−1 puromycin for 48 h and clones were isolated by limiting dilution. Clones were
683 selected for their absence of Crk expression by Western blot. One clone was selected for
684 further experiments.

685 ***crk* sequence analysis in Crk-deficient cells**

686 Genomic DNA was isolated from 4.10^6 NCI-H292 and Crk-deficient cells using the DNeasy®
687 Blood & Tissue kit (Qiagen, #69504) and following the manufacturer's protocol. The *crk* gene
688 was amplified by PCR using 100 ng of gDNA from each cell line with primers PCR-Crk_F and
689 PCR-Crk_R (Supplementary Table 2). PCR fragments were then purified and sent for Sanger
690 sequencing with Seq-Crk_F and Seq-Crk_R and TIDE software was used to analyze indels in the
691 *crk* gene from Crk-deficient cells.

692 **Complementation of Crk-deficient cells**

693 The *CrkI* and *CrkII* genes were synthetized by Twist Bioscience and cloned into the pTwist Amp
694 High Copy plasmid (2221 bp). Some modifications have been introduced, that did not result in
695 changes of the amino acid sequence, to prevent the Cas9 endonuclease from cleaving the
696 gene after its insertion into the genome of deficient cells, and to reduce the %GC content for
697 gene synthesis. Moreover, XbaI and BamHI restriction sites were added at 5' and 3' ends of
698 each gene, respectively (Supplementary Table 3). Each gene was next cloned into XbaI/BamHI-
699 digested pLVX-IRES-neo vector. Lentiviral particles containing the pLVX-neo_CrkI or pLVX-
700 neo_CrkII plasmid were then produced as previously described. Thereafter, Crk-deficient cells
701 were incubated with lentiviral particles under the same conditions as described above with
702 geneticin selection, and stable cell lines derived from Crk-deficient cells but expressing CrkI or
703 CrkII were selected by limiting dilution. Genomic DNA from each selected clone was extracted
704 using the DNeasy® Blood & Tissue kit (Qiagen, #69504) and primers VD20_F and VD20_R were
705 used for PCR amplification of the modified *crk* gene and sequencing. Selected clones were also
706 tested by WB for CrkI and CrkII expression.

707 **Cell retraction assay**

708 $1,3.10^4$ NCI-H292 cells or their derivatives were seeded per well in a 96-well plate (Greiner,
709 #655090) 48h before infection ($1,3.10^4$ HeLa cells or $1,5.10^4$ A549 cells). For the cell retraction
710 assay, cells were first labeled with Cytotrace Red CMTPX (1µM) for one hour in their FBS-

711 containing culture medium, to label cell cytoplasm after which the medium was removed and
712 replaced with phenol red-free RPMI medium (Gibco, #32404014) supplemented with
713 GlutaMAX (Gibco, #35050038). Cells were subsequently infected at MOI 20 with bacteria
714 (unless otherwise indicated). The total cell area was monitored using an IncuCyte live-Cell
715 microscope (SX5, Sartorius) containing the Green/Red module. Images from bright field
716 (phase) and red channel (acquisition time 400 ms) were collected every 15 min for 12 h using
717 a x10 objective and treated using the IncuCyte software.
718 For the quantification of cell retraction induced by the GAP and ADPRT domains of ExoS and
719 ExoT toxins, the same protocol was used with the exception that the analysis was performed
720 using images acquired with Incucyte (images with the red channel) at a given point and using
721 the Analyze Particles module from FIJI.

722 **Western Blot (WB) analysis**

723 Cells were seeded at 4.10^5 cells per well in a 6-well plate and incubated for 2 days (2.10^4 A549
724 or HeLa cells). Next, cells were quantified and infected at the indicated MOI and time, then
725 washed twice with cold PBS before freezing. Cells were lysed with lysis buffer containing 1%
726 Triton X-100, 50mM Tris-HCl pH 7.4, 150mM NaCl, 1mM EDTA, and Roche protease inhibitor
727 cocktail. The lysates were incubated 15 min on ice and centrifuged at 12,000 g for 15 min at
728 4°C and protein concentration in the supernatant was measured using the Bradford assay.
729 Thirty micrograms of protein were then denatured with a buffer containing LDS (Invitrogen,
730 #NP0007) and a reducing agent (Bio-Rad, #1610792) at 95 °C for 5 min. For gel electrophoresis,
731 proteins were run using NuPAGE 4-12% Bis-Tris gels (Invitrogen, #NP0321BOX) and the MES
732 SDS Running buffer (Invitrogen, #NP0002). Proteins were then transferred onto a PVDF
733 membrane, using wet transfer in a transfer cell for 1h at 4°C and 350 mA. Finally, the blots
734 were saturated with detergent-containing Tris-buffered saline (TBST) supplemented with 5%
735 BSA. The TBST wash buffer consists of 10 mM Tris pH 7.5, 150 mM NaCl and 0.05% Tween® 20
736 detergent. The saturation step was carried out for 90 min at room temperature, and the blots
737 were washed three times for 5 minutes each with the TBST buffer before being incubated
738 overnight at 4°C with the primary antibodies. After three washes, primary antibodies were
739 probed using an HRP-labeled detection antibody for 90 min at room temperature. Then blots
740 were washed three times and signals were detected using the SuperSignal West Pico PLUS

741 Chemiluminescent Substrate (ThermoScientific, #34577) and the ChemiDoc MP Imaging
742 System.
743 For the visualization of phospho-CrkII at different time-point, similar experiment was
744 performed but NCI-H292 cells were seeded at $2,5.10^5$ cells per well in a 12-well plate. The cells
745 were then infected at the corresponding times and lysed with a lysis buffer containing 1%
746 Triton X-100, 50mM Tris-HCl pH 7.4, 150mM NaCl, 5mM EDTA, and 1X Halt Protease &
747 Phosphatase Inhibitor Cocktail (Thermo Fisher Scientific, #1861281). When indicated,
748 Spermine NONOate was added to each infected well at 50 µM at the time of infection. Wells
749 infected for 2h or more received a further 50 µM Spermine NONOate for 2h. 8-Br-cGMP was
750 added for 5h at 500 µM to dedicated infected wells (i.e., 1h30 before the start of infection)
751 and wells with 2h30 or more of infection received a further 500 µM 8-Br-cGMP for 2h30.
752 For secretion of T3SS effectors, overnight cultures of the PAO1FΔS and PAO1FΔT strains were
753 diluted to 0.05 and grown for 3 h in LB supplemented with 5 mM EGTA and 20 mM $MgCl_2$ to
754 reach an OD of 1. Then, 1 ml of each culture was centrifuged to pellet the bacteria and the
755 supernatant was harvested and mixed with 10 µl of 10% Triton X-100 (0.1% final
756 concentration) before being flash frozen. Finally, 14 µL of each of the supernatants (containing
757 T3SS effectors) were denatured with buffer containing LDS and reducing agent and ran using
758 NuPAGE 4-12% Bis-Tris gels for gel electrophoresis.

759 **Statistics**

760 GraphPad software (version 9.5.1) was used for statistical analyses. For cytotoxicity assays,
761 AUC was extracted from each retraction curve and plotted on a bar chart. A one-way ANOVA
762 was employed, followed by Tukey's post-hoc test for data comparison. The same statistical
763 method was used to analyze the maximum luminescence of transfected or infected cells
764 expressing cGMP or cAMP GloSensor, the production of cGMP and cAMP in infected cells by
765 ELISA, and the cell retraction induced by ExoS and ExoT domains. For the statistical analysis of
766 guanylate, adenylate, uridylyl and cytidylyl cyclase activities of purified proteins, the same
767 method was applied except that a Dunnett's post-hoc test was performed using the sample
768 with ExoY WT as control. Statistical differences in CrkII phosphorylation levels between 2 and
769 3h were established using a Fisher's LSD test. Finally, statistical analysis of Fig2B was
770 performed using an unpaired two-tailed t-test.

771 **AUTHOR CONTRIBUTIONS:**

772 V.D., U.M. and L.R. contributed to the conception and design of the study. V.D. performed all
773 the experiments and analyzed data. G.D. participated in the ELISA experiments and D.R.B. in
774 the *in vitro* measurements of cNMPs. E.L. was involved in generating deficient cells and
775 modifying the ADPRT domain of ExoT. V. D. and R.P.L. infected the cGMP reporter cell line.
776 V.D. wrote the manuscript. V.D., U.M., D.L. and L.R. edited the manuscript. All authors
777 approved the final manuscript.

778 **FUNDING:**

779 This project was funded by the ANR under #ANR-18-CE44-0004 (activExoY) and under #ANR-
780 23-CE44-0047 (toxi-cUMPsignal) and by CNRS UMR 3528. V.D. was supported by Pasteur-
781 Roux-Cantarini program and E.L. by a stipend from Amgen Scholars Program. G.D. received a
782 doctoral fellowship from the French Ministry of Higher Education, Research, and Innovation.
783 R.P.L. was supported by a stipend from the Pasteur—Paris University (PPU) International PhD
784 Program.

785 **ACKNOWLEDGEMENT:**

786 We thank Arne Rietsch (Case Western Reserve University, Ohio), for providing the indicated
787 *P. aeruginosa* strains used in this study and the ExoS and ExoT antibodies. We also thank Éric
788 Faudry and Ina Attrée (IBS, Grenoble) for access to the PAO1F mutant strains. We thank Stefan
789 Dove for his advice on modifying the substrate specificity of ExoY, Alexander Belyy for his
790 preliminary work on ExoY substrate specificity and Magda Teixeira-Nunes and Martine
791 Comisso for their technical assistance in designing the ExoY variants. We would also like to
792 thank Alexandre Chenal for the CyaA proteins.

REFERENCES:

1. Reynolds, D. & Kollef, M. The Epidemiology and Pathogenesis and Treatment of Pseudomonas aeruginosa Infections: An Update. *Drugs* **81**, 2117–2131 (2021).
2. Qin, S. *et al.* Pseudomonas aeruginosa: pathogenesis, virulence factors, antibiotic resistance, interaction with host, technology advances and emerging therapeutics. *Signal Transduct. Target. Ther.* **7**, 1–27 (2022).
3. Franzetti, F., Cernuschi, M., Esposito, R. & Moroni, M. Pseudomonas infections in patients with AIDS and AIDS-related complex. *J. Intern. Med.* **231**, 437–443 (1992).
4. Bhagirath, A. Y. *et al.* Cystic fibrosis lung environment and Pseudomonas aeruginosa infection. *BMC Pulm. Med.* **16**, 174 (2016).
5. Davies, J. C. *Pseudomonas aeruginosa* in cystic fibrosis: pathogenesis and persistence. *Paediatr. Respir. Rev.* **3**, 128–134 (2002).
6. Zhang, Y. *et al.* Risk Factors for Mortality of Inpatients with Pseudomonas aeruginosa Bacteremia in China: Impact of Resistance Profile in the Mortality. *Infect. Drug Resist.* **13**, 4115–4123 (2020).
7. Anantharajah, A., Mingeot-Leclercq, M.-P. & Van Bambeke, F. Targeting the Type Three Secretion System in *Pseudomonas aeruginosa*. *Trends Pharmacol. Sci.* **37**, 734–749 (2016).
8. Juan, C., Peña, C. & Oliver, A. Host and Pathogen Biomarkers for Severe Pseudomonas aeruginosa Infections. *J. Infect. Dis.* **215**, S44–S51 (2017).
9. Engel, J. & Balachandran, P. Role of *Pseudomonas aeruginosa* type III effectors in disease. *Curr. Opin. Microbiol.* **12**, 61–66 (2009).
10. Hauser, A. R. The type III secretion system of Pseudomonas aeruginosa: infection by injection. *Nat. Rev. Microbiol.* **7**, 654–665 (2009).
11. Karlberg, T. *et al.* 14-3-3 proteins activate Pseudomonas exotoxins-S and -T by chaperoning a hydrophobic surface. *Nat. Commun.* **9**, 3785 (2018).
12. Zhang, A., Veesenmeyer, J. L. & Hauser, A. R. Phosphatidylinositol 4,5-Bisphosphate-Dependent Oligomerization of the Pseudomonas aeruginosa Cytotoxin ExoU. *Infect. Immun.* **86**, e00402-17 (2017).
13. Deruelle, V. *et al.* The bacterial toxin ExoU requires a host trafficking chaperone for transportation and to induce necrosis. *Nat. Commun.* **12**, 4024 (2021).
14. Belyy, A. *et al.* Actin activates Pseudomonas aeruginosa ExoY nucleotidyl cyclase toxin and ExoY-like effector domains from MARTX toxins. *Nat. Commun.* **7**, 13582 (2016).
15. Feltman, H. *et al.* Prevalence of type III secretion genes in clinical and environmental isolates of Pseudomonas aeruginosa. *Microbiology* **147**, 2659–2669 (2001).
16. Ozer, E. A., Nnah, E., Didelot, X., Whitaker, R. J. & Hauser, A. R. The Population Structure of Pseudomonas aeruginosa Is Characterized by Genetic Isolation of exoU+ and exoS+ Lineages. *Genome Biol. Evol.* **11**, 1780–1796 (2019).
17. Horna, G., Amaro, C., Palacios, A., Guerra, H. & Ruiz, J. High frequency of the exoU+/exoS+ genotype associated with multidrug-resistant “high-risk clones” of Pseudomonas aeruginosa clinical isolates from Peruvian hospitals. *Sci. Rep.* **9**, 10874 (2019).
18. Song, Y. *et al.* Emergence of hypervirulent *Pseudomonas aeruginosa* pathotypically armed with co-expressed T3SS effectors ExoS and ExoU. *hLife* **1**, 44–56 (2023).
19. Morales-Espinosa, R. *et al.* Fingerprint Analysis and Identification of Strains ST309 as a Potential High Risk Clone in a Pseudomonas aeruginosa Population Isolated from Children with Bacteremia in Mexico City. *Front. Microbiol.* **8**, (2017).
20. Yahr, T. L., Vallis, A. J., Hancock, M. K., Barbieri, J. T. & Frank, D. W. ExoY, an

840 adenylate cyclase secreted by the Pseudomonas aeruginosa type III system. *Proc. Natl. Acad.*
841 *Sci. U. S. A.* **95**, 13899–13904 (1998).
842 21. Ochoa, C. D., Alexeyev, M., Pastukh, V., Balczon, R. & Stevens, T. Pseudomonas
843 aeruginosa Exotoxin Y Is a Promiscuous Cyclase That Increases Endothelial Tau
844 Phosphorylation and Permeability. *J. Biol. Chem.* **287**, 25407–25418 (2012).
845 22. Raoux-Barbot, D. *et al.* Differential regulation of actin-activated nucleotidyl cyclase
846 virulence factors by filamentous and globular actin. *PloS One* **13**, e0206133 (2018).
847 23. Belyy, A., Merino, F., Mechold, U. & Raunser, S. Mechanism of actin-dependent
848 activation of nucleotidyl cyclase toxins from bacterial human pathogens. *Nat. Commun.* **12**,
849 6628 (2021).
850 24. Teixeira Nunes, M. *et al.* Functional and structural insights into the multi-step
851 activation and catalytic mechanism of bacterial ExoY nucleotidyl cyclase toxins bound to
852 actin-profilin. *PLoS Pathog.* **19**, e1011654 (2023).
853 25. Teixeira-Nunes, M. *et al.* Bacterial Nucleotidyl Cyclases Activated by Calmodulin or
854 Actin in Host Cells: Enzyme Specificities and Cytotoxicity Mechanisms Identified to Date. *Int.*
855 *J. Mol. Sci.* **23**, 6743 (2022).
856 26. Khanppnavar, B. & Datta, S. Crystal structure and substrate specificity of ExoY, a
857 unique T3SS mediated secreted nucleotidyl cyclase toxin from *Pseudomonas aeruginosa*.
858 *Biochim. Biophys. Acta BBA - Gen. Subj.* **1862**, 2090–2103 (2018).
859 27. Beckert, U. *et al.* ExoY from Pseudomonas aeruginosa is a nucleotidyl cyclase with
860 preference for cGMP and cUMP formation. *Biochem. Biophys. Res. Commun.* **450**, 870–874
861 (2014).
862 28. Beste, K. Y. *et al.* Nucleotidyl Cyclase Activity of Particulate Guanylyl Cyclase A:
863 Comparison with Particulate Guanylyl Cyclases E and F, Soluble Guanylyl Cyclase and
864 Bacterial Adenylyl Cyclases Cyaa and Edema Factor. *PLoS ONE* **8**, e70223 (2013).
865 29. Schulert, G. S. *et al.* Secretion of the Toxin ExoU Is a Marker for Highly Virulent
866 Pseudomonas aeruginosa Isolates Obtained from Patients with Hospital-Acquired
867 Pneumonia. *J. Infect. Dis.* **188**, 1695–1706 (2003).
868 30. Silistre, H. *et al.* Prevalence of ExoY Activity in Pseudomonas aeruginosa Reference
869 Panel Strains and Impact on Cytotoxicity in Epithelial Cells. *Front. Microbiol.* **12**, 666097
870 (2021).
871 31. Wolfgang, M. C. *et al.* Conservation of genome content and virulence determinants
872 among clinical and environmental isolates of Pseudomonas aeruginosa. *Proc. Natl. Acad. Sci.*
873 *U. S. A.* **100**, 8484–8489 (2003).
874 32. Vallis, A. J., Finck-Barbançon, V., Yahr, T. L. & Frank, D. W. Biological Effects of
875 Pseudomonas aeruginosa Type III-Secreted Proteins on CHO Cells. *Infect. Immun.* **67**, 2040–
876 2044 (1999).
877 33. Balczon, R. *et al.* Pseudomonas aeruginosa Exotoxin Y-Mediated Tau
878 Hyperphosphorylation Impairs Microtubule Assembly in Pulmonary Microvascular
879 Endothelial Cells. *PLoS ONE* **8**, e74343 (2013).
880 34. Stevens, T. C. *et al.* The Pseudomonas aeruginosa exoenzyme Y impairs endothelial
881 cell proliferation and vascular repair following lung injury. *Am. J. Physiol. - Lung Cell. Mol.*
882 *Physiol.* **306**, L915–L924 (2014).
883 35. Morrow, K. A. *et al.* Heterogeneity of pulmonary endothelial cyclic nucleotide
884 response to Pseudomonas aeruginosa ExoY infection. *Am. J. Physiol. - Lung Cell. Mol. Physiol.*
885 **309**, L1199–L1207 (2015).
886 36. Morrow, K. A. *et al.* Pseudomonas aeruginosa exoenzymes U and Y induce a

887 transmissible endothelial proteinopathy. *Am. J. Physiol. - Lung Cell. Mol. Physiol.* **310**, L337–
888 L353 (2016).
889 37. Sayner, S. L. *et al.* Paradoxical cAMP-Induced Lung Endothelial Hyperpermeability
890 Revealed by Pseudomonas aeruginosa ExoY. *Circ. Res.* **95**, 196–203 (2004).
891 38. Lee, V. T., Smith, R. S., Tümmler, B. & Lory, S. Activities of Pseudomonas aeruginosa
892 Effectors Secreted by the Type III Secretion System In Vitro and during Infection. *Infect.*
893 *Immun.* **73**, 1695–1705 (2005).
894 39. Ganter, M. T. *et al.* Role of Small GTPases and αvβ5 Integrin in Pseudomonas
895 aeruginosa–Induced Increase in Lung Endothelial Permeability. *Am. J. Respir. Cell Mol. Biol.*
896 **40**, 108–118 (2009).
897 40. Huber, P., Bouillot, S., Elsen, S. & Attrée, I. Sequential inactivation of Rho GTPases
898 and Lim kinase by Pseudomonas aeruginosa toxins ExoS and ExoT leads to endothelial
899 monolayer breakdown. *Cell. Mol. Life Sci. CMLS* **71**, 1927–1941 (2013).
900 41. Munder, A. *et al.* The Pseudomonas aeruginosa ExoY phenotype of high-copy-number
901 recombinants is not detectable in natural isolates. *Open Biol.* **8**, 170250 (2018).
902 42. Ichikawa, J. K. *et al.* Genome-wide analysis of host responses to the Pseudomonas
903 aeruginosa type III secretion system yields synergistic effects. *Cell. Microbiol.* **7**, 1635–1646
904 (2005).
905 43. Bouillot, S., Attrée, I. & Huber, P. Pharmacological Activation of Rap1 Antagonizes the
906 Endothelial Barrier Disruption Induced by Exotoxins ExoS and ExoT of Pseudomonas
907 aeruginosa. *Infect. Immun.* **83**, 1820–1829 (2015).
908 44. Vance, R. E., Rietsch, A. & Mekalanos, J. J. Role of the Type III Secreted Exoenzymes S,
909 T, and Y in Systemic Spread of Pseudomonas aeruginosa PAO1 In Vivo. *Infect. Immun.* **73**,
910 1706–1713 (2005).
911 45. Armentrout, E. I., Kundracik, E. C. & Rietsch, A. Cell-type-specific hypertranslocation
912 of effectors by the Pseudomonas aeruginosa type III secretion system. *Mol. Microbiol.* **115**,
913 305–319 (2021).
914 46. Cisz, M., Lee, P.-C. & Rietsch, A. ExoS Controls the Cell Contact-Mediated Switch to
915 Effector Secretion in Pseudomonas aeruginosa. *J. Bacteriol.* **190**, 2726–2738 (2008).
916 47. Pederson, K. J., Vallis, A. J., Aktories, K., Frank, D. W. & Barbieri, J. T. The amino-
917 terminal domain of Pseudomonas aeruginosa ExoS disrupts actin filaments via small-
918 molecular-weight GTP-binding proteins. *Mol. Microbiol.* **32**, 393–401 (1999).
919 48. Maresso, A. W., Baldwin, M. R. & Barbieri, J. T. Ezrin/Radixin/Moesin Proteins Are
920 High Affinity Targets for ADP-ribosylation by *Pseudomonas aeruginosa* ExoS*. *J. Biol. Chem.*
921 **279**, 38402–38408 (2004).
922 49. Kazmierczak, B. I. & Engel, J. N. Pseudomonas aeruginosa ExoT Acts In Vivo as a
923 GTPase-Activating Protein for RhoA, Rac1, and Cdc42. *Infect. Immun.* **70**, 2198–2205 (2002).
924 50. Garrity-Ryan, L. *et al.* The ADP Ribosyltransferase Domain of Pseudomonas
925 aeruginosa ExoT Contributes to Its Biological Activities. *Infect. Immun.* **72**, 546–558 (2004).
926 51. Garrity-Ryan, L. *et al.* The Arginine Finger Domain of ExoT Contributes to Actin
927 Cytoskeleton Disruption and Inhibition of Internalization of Pseudomonas aeruginosa by
928 Epithelial Cells and Macrophages. *Infect. Immun.* **68**, 7100–7113 (2000).
929 52. Goehring, U. M., Schmidt, G., Pederson, K. J., Aktories, K. & Barbieri, J. T. The N-
930 terminal domain of Pseudomonas aeruginosa exoenzyme S is a GTPase-activating protein for
931 Rho GTPases. *J. Biol. Chem.* **274**, 36369–36372 (1999).
932 53. Deng, Q. & Barbieri, J. T. Modulation of host cell endocytosis by the type-III cytotoxin,
933 Pseudomonas ExoS. *Traffic Cph. Den.* **9**, 1948–1957 (2008).

934 54. Würtele, M., Renault, L., Barbieri, J. T., Wittinghofer, A. & Wolf, E. Structure of the
935 ExoS GTPase activating domain. *FEBS Lett.* **491**, 26–29 (2001).
936 55. Radke, J., Pederson, K. J. & Barbieri, J. T. Pseudomonas aeruginosa Exoenzyme S Is a
937 Biglutamic Acid ADP-Ribosyltransferase. *Infect. Immun.* **67**, 1508–1510 (1999).
938 56. Wood, S. J., Goldufsky, J. W., Bello, D., Masood, S. & Shafikhani, S. H. Pseudomonas
939 aeruginosa ExoT Induces Mitochondrial Apoptosis in Target Host Cells in a Manner That
940 Depends on Its GTPase-activating Protein (GAP) Domain Activity. *J. Biol. Chem.* **290**, 29063–
941 29073 (2015).
942 57. Sundin, C., Hallberg, B. & Forsberg, A. ADP-ribosylation by exoenzyme T of
943 Pseudomonas aeruginosa induces an irreversible effect on the host cell cytoskeleton in vivo.
944 *FEMS Microbiol. Lett.* **234**, 87–91 (2004).
945 58. Minns, M. S. *et al.* NLRP3 selectively drives IL-1β secretion by Pseudomonas
946 aeruginosa infected neutrophils and regulates corneal disease severity. *Nat. Commun.* **14**,
947 5832 (2023).
948 59. Krall, R., Schmidt, G., Aktories, K. & Barbieri, J. T. Pseudomonas aeruginosa ExoT Is a
949 Rho GTPase-Activating Protein. *Infect. Immun.* **68**, 6066–6068 (2000).
950 60. Ganesan, A. K., Frank, D. W., Misra, R. P., Schmidt, G. & Barbieri, J. T. *Pseudomonas*
951 *aeruginosa* Exoenzyme S ADP-ribosylates Ras at Multiple Sites*. *J. Biol. Chem.* **273**, 7332–
952 7337 (1998).
953 61. Ganesan, A. K., Vincent, T. S., Olson, J. C. & Barbieri, J. T. *Pseudomonas aeruginosa*
954 Exoenzyme S Disrupts Ras-mediated Signal Transduction by Inhibiting Guanine Nucleotide
955 Exchange Factor-catalyzed Nucleotide Exchange*. *J. Biol. Chem.* **274**, 21823–21829 (1999).
956 62. Fraylick, J. E., Riese, M. J., Vincent, T. S., Barbieri, J. T. & Olson, J. C. ADP-Ribosylation
957 and Functional Effects of Pseudomonas Exoenzyme S on Cellular RalA. *Biochemistry* **41**,
958 9680–9687 (2002).
959 63. Henriksson, M. L. *et al.* Exoenzyme S shows selective ADP-ribosylation and GTPase-
960 activating protein (GAP) activities towards small GTPases in vivo. *Biochem. J.* **367**, 617–628
961 (2002).
962 64. Fraylick, J. E., Rucks, E. A., Greene, D. M., Vincent, T. S. & Olson, J. C. Eukaryotic Cell
963 Determination of ExoS ADP-Ribosyltransferase Substrate Specificity. *Biochem. Biophys. Res.*
964 *Commun.* **291**, 91–100 (2002).
965 65. Riese, M. J., Wittinghofer, A. & Barbieri, J. T. ADP Ribosylation of Arg41 of Rap by
966 ExoS Inhibits the Ability of Rap To Interact with Its Guanine Nucleotide Exchange Factor,
967 C3G. *Biochemistry* **40**, 3289–3294 (2001).
968 66. Sun, J. & Barbieri, J. T. *Pseudomonas aeruginosa* ExoT ADP-ribosylates CT10 Regulator
969 of Kinase (Crk) Proteins*. *J. Biol. Chem.* **278**, 32794–32800 (2003).
970 67. Barbieri, J. T. & Sun, J. Pseudomonas aeruginosa ExoS and ExoT. in *Reviews of*
971 *Physiology, Biochemistry and Pharmacology* 79–92 (Springer, Berlin, Heidelberg, 2005).
972 doi:10.1007/s10254-004-0031-7.
973 68. Ebenwaldner, C. *et al.* 14-3-3 Activated Bacterial Exotoxins AexT and ExoT Share Actin
974 and the SH2 Domains of CRK Proteins as Targets for ADP-Ribosylation. *Pathogens* **11**, 1497
975 (2022).
976 69. Deng, Q., Sun, J. & Barbieri, J. T. Uncoupling Crk signal transduction by Pseudomonas
977 exoenzyme T. *J. Biol. Chem.* **280**, 35953–35960 (2005).
978 70. Birge, R. B., Kalodimos, C., Inagaki, F. & Tanaka, S. Crk and CrkL adaptor proteins:
979 networks for physiological and pathological signaling. *Cell Commun. Signal. CCS* **7**, 13 (2009).
980 71. Martinez-Quiles, N., Feuerbacher, L. A., Benito-León, M. & Hardwidge, P. R.

981 Contribution of Crk Adaptor Proteins to Host Cell and Bacteria Interactions. *BioMed Res. Int.*
982 **2014**, 372901 (2014).
983 72. Feller, S. M., Knudsen, B. & Hanafusa, H. c-Abl kinase regulates the protein binding
984 activity of c-Crk. *EMBO J.* **13**, 2341–2351 (1994).
985 73. Pielage, J. F., Powell, K. R., Kalman, D. & Engel, J. N. RNAi screen reveals an Abl
986 kinase-dependent host cell pathway involved in Pseudomonas aeruginosa internalization.
987 *PLoS Pathog.* **4**, e1000031 (2008).
988 74. Shishido, T. *et al.* Crk family adaptor proteins trans-activate c-Abl kinase. *Genes Cells*
989 **6**, 431–440 (2001).
990 75. Ren, R., Ye, Z. S. & Baltimore, D. Abl protein-tyrosine kinase selects the Crk adapter as
991 a substrate using SH3-binding sites. *Genes Dev.* **8**, 783–795 (1994).
992 76. Abassi, Y. A. & Vuori, K. Tyrosine 221 in Crk regulates adhesion-dependent membrane
993 localization of Crk and Rac and activation of Rac signaling. *EMBO J.* **21**, 4571 (2002).
994 77. Klemke, R. L. *et al.* CAS/Crk Coupling Serves as a "Molecular Switch" for Induction of
995 Cell Migration. *J. Cell Biol.* **140**, 961–972 (1998).
996 78. Albert, M. L., Kim, J.-I. & Birge, R. B. αvβ5 integrin recruits the CrkII–Dock180–Rac1
997 complex for phagocytosis of apoptotic cells. *Nat. Cell Biol.* **2**, 899–905 (2000).
998 79. Nakashima, N. *et al.* The Functional Role of CrkII in Actin Cytoskeleton Organization
999 and Mitogenesis*. *J. Biol. Chem.* **274**, 3001–3008 (1999).
1000 80. Matsuda, M. & Kurata, T. Emerging components of the Crk oncogene product: The
1001 first identified adaptor protein. *Cell. Signal.* **8**, 335–340 (1996).
1002 81. Kiyokawa, E., Hashimoto, Y., Kurata, T., Sugimura, H. & Matsuda, M. Evidence That
1003 DOCK180 Up-regulates Signals from the CrkII-p130Cas Complex *. *J. Biol. Chem.* **273**, 24479–
1004 24484 (1998).
1005 82. Birge, R. B., Fajardo, J. E., Mayer, B. J. & Hanafusa, H. Tyrosine-phosphorylated
1006 epidermal growth factor receptor and cellular p130 provide high affinity binding substrates
1007 to analyze Crk-phosphotyrosine-dependent interactions in vitro. *J. Biol. Chem.* **267**, 10588–
1008 10595 (1992).
1009 83. Kain, K. H., Gooch, S. & Klemke, R. L. Cytoplasmic c-Abl provides a molecular
1010 'Rheostat' controlling carcinoma cell survival and invasion. *Oncogene* **22**, 6071–6080 (2003).
1011 84. Holcomb, M., Rufini, A., Barilà, D. & Klemke, R. L. Deregulation of proteasome
1012 function induces Abl-mediated cell death by uncoupling p130CAS and c-CrkII. *J. Biol. Chem.*
1013 **281**, 2430–2440 (2006).
1014 85. Takino, T. *et al.* Tyrosine phosphorylation of the CrkII adaptor protein modulates cell
1015 migration. *J. Cell Sci.* **116**, 3145–3155 (2003).
1016 86. Chodniewicz, D. & Klemke, R. L. Regulation of integrin-mediated cellular responses
1017 through assembly of a CAS/Crk scaffold. *Biochim. Biophys. Acta BBA - Mol. Cell Res.* **1692**,
1018 63–76 (2004).
1019 87. Mohamed, M. F. *et al.* CrkII/Abl phosphorylation cascade is critical for NLRC4
1020 inflammasome activity and is blocked by Pseudomonas aeruginosa ExoT. *Nat. Commun.* **13**,
1021 1295 (2022).
1022 88. Wood, S., Goldufsky, J. & Shafikhani, S. H. Pseudomonas aeruginosa ExoT Induces
1023 Atypical Anoikis Apoptosis in Target Host Cells by Transforming Crk Adaptor Protein into a
1024 Cytotoxin. *PLoS Pathog.* **11**, e1004934 (2015).
1025 89. Shafikhani, S. H., Morales, C. & Engel, J. The Pseudomonas aeruginosa type III
1026 secreted toxin ExoT is necessary and sufficient to induce apoptosis in epithelial cells. *Cell.*
1027 *Microbiol.* **10**, 994–1007 (2008).

1028 90. Ros, O. *et al.* SponGee: A Genetic Tool for Subcellular and Cell-Specific cGMP
1029 Manipulation. *Cell Rep.* **27**, 4003-4012.e6 (2019).
1030 91. Liu, F. & Chernoff, J. Protein tyrosine phosphatase 1B interacts with and is tyrosine
1031 phosphorylated by the epidermal growth factor receptor. *Biochem. J.* **327 (Pt 1)**, 139–145
1032 (1997).
1033 92. Hernández-Sotomayor, S. M., Arteaga, C. L., Soler, C. & Carpenter, G. Epidermal
1034 growth factor stimulates substrate-selective protein-tyrosine-phosphatase activity. *Proc.*
1035 *Natl. Acad. Sci.* **90**, 7691–7695 (1993).
1036 93. Lan, T. *et al.* Increased endogenous PKG I activity attenuates EGF-induced
1037 proliferation and migration of epithelial ovarian cancer via the MAPK/ERK pathway. *Cell*
1038 *Death Dis.* **14**, 1–12 (2023).
1039 94. Lan, T. *et al.* Type II cGMP-dependent protein kinase phosphorylates EGFR at
1040 threonine 669 and thereby inhibits its activation. *Biochem. Biophys. Res. Commun.* **518**, 14–
1041 18 (2019).
1042 95. Jiang, L. *et al.* PKG II Inhibits EGF/EGFR-Induced Migration of Gastric Cancer Cells.
1043 *PLOS ONE* **8**, e61674 (2013).
1044 96. Wu, Y. *et al.* PKG II secreted via the classical endoplasmic reticulum–Golgi apparatus
1045 secretory pathway blocks the activation of EGFR through phosporalting its threonine 406
1046 and has an anti-tumor effect. *Front. Biosci.-Landmark* **27**, 53 (2022).
1047 97. Hmelo, L. R. *et al.* Precision-engineering the Pseudomonas aeruginosa genome with
1048 two-step allelic exchange. *Nat. Protoc.* **10**, 1820–1841 (2015).
1049 98. Voegele, A. *et al.* A High-Affinity Calmodulin-Binding Site in the CyaA Toxin
1050 Translocation Domain is Essential for Invasion of Eukaryotic Cells. *Adv. Sci.* **8**, 2003630
1051 (2021).

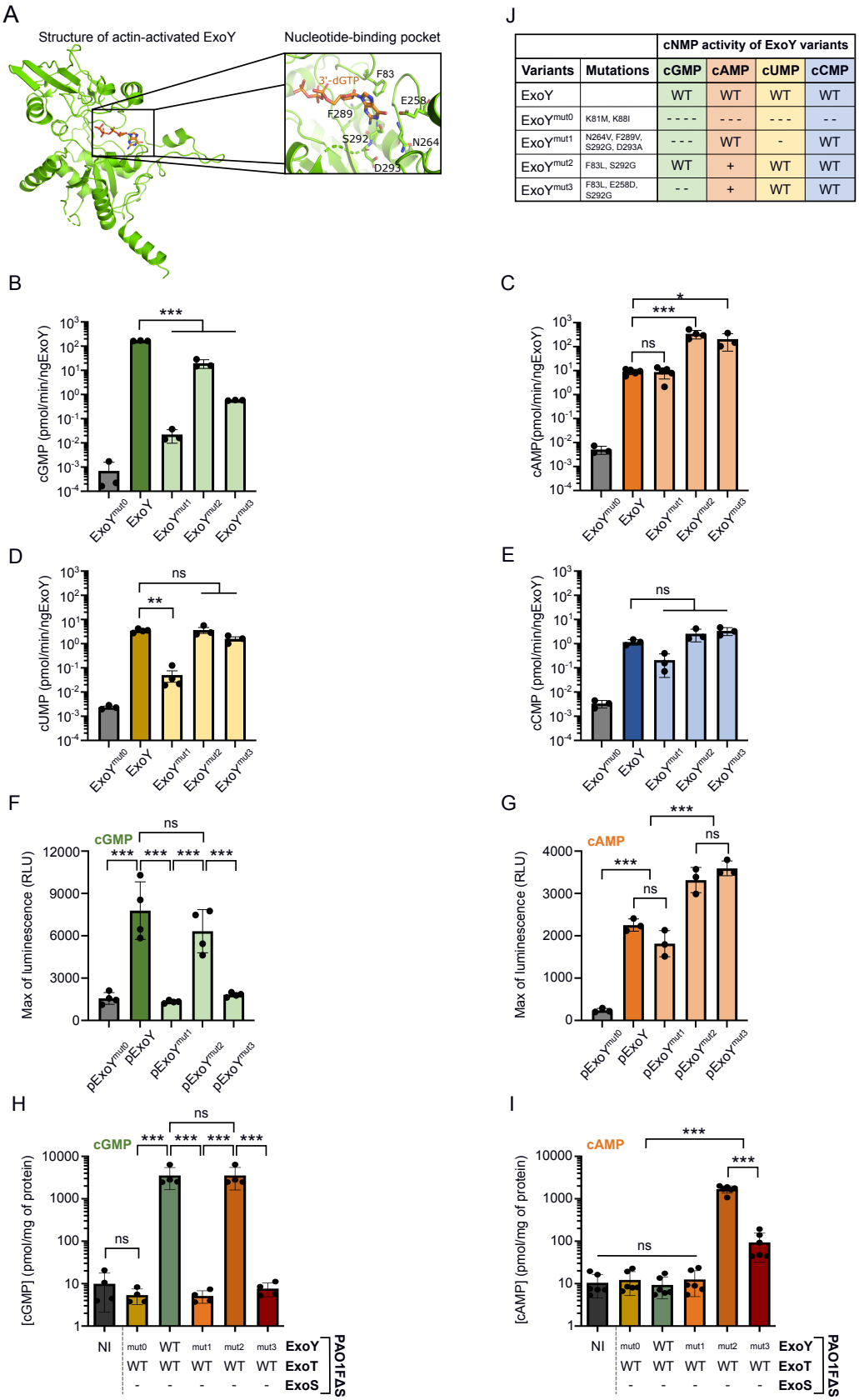

		cNMP activity of ExoY variants			
Variants	**Mutations**	**cGMP**	**cAMP**	**cUMP**	**cCMP**
ExoY		WT	WT	WT	WT
ExoY^{mut0}	K81M, K88I	- - - -	- - -	- - -	- -
ExoY^{mut1}	N264V, F289V, S292G, D293A	- - -	WT	-	WT
ExoY^{mut2}	F83L, S292G	WT	+	WT	WT
ExoY^{mut3}	F83L, E258D, S292G	- -	+	WT	WT

Figure 1: Modification of ExoY effector substrate specificity.

A. Structure of the *Pseudomonas aeruginosa* ExoY bound to F-actin and 3'-deoxy GTP (3'-dGTP) as solved by *Belyy* et *al.*,[1] with a detailed view of its nucleotide-binding pocket. Modified

residues to change ExoY's substrate specificity are highlighted. **B.** Analysis of guanylate cyclase (GC) activity, **C.** adenylate cyclase (AC), **D.** uridylyl cyclase and **E.** cytidylyl cyclase activities of purified ExoY proteins. Statistical differences were established by one way ANOVA, followed by Dunnett's multiple comparison test with ExoY as a control group (*p = 0.033, **p = 0.002, ***p < 0.001, n.s., non-significant). **F.** Luminescence activity of the cGMP- or **G.** cAMP-GloSensor reporter cell line. Stable cell lines were co-transfected with an expression plasmid encoding an ExoY variant and the Tet-On 3G transactivator expression plasmid. Cells were incubated with 1 µM of Doxycycline for 3 h prior recording luminescence intensity. The luminescence maximum was extracted and plotted. **H.** Quantification of cGMP or **I.** cAMP production in NCI-H292 cells by ELISA after 5h or 3h of infection respectively, at MOI 20 with PAO1FΔS strains. Statistical differences were established by one way ANOVA, followed by Tukey's test (*p = 0.033, **p = 0.002, ***p < 0.001, n.s., non-significant). **J.** Summary table of the activity of each ExoY variant to produce different cNMPs. A scale corresponding to the magnitude of the fold change (FC) obtained with purified ExoY proteins (cNMP production by ExoY variants compared to ExoY WT) is represented as follows: WT indicates that cNMP production is similar to that of ExoY WT (10^{-1}<FC<10^{1}). -/+ means that NC activity is decreased/ increased compared to ExoY WT with "-" for a FC magnitude between 10-100, "- - " for a FC magnitude between 100-1,000; " - - -" between 1,000-10,000, " - - - -" if greater than 10,000, and the same with + for increased NC activity. The results of plasmid expressions in luminescent reporter cells and ELISA assays after infection agree with the summary table.

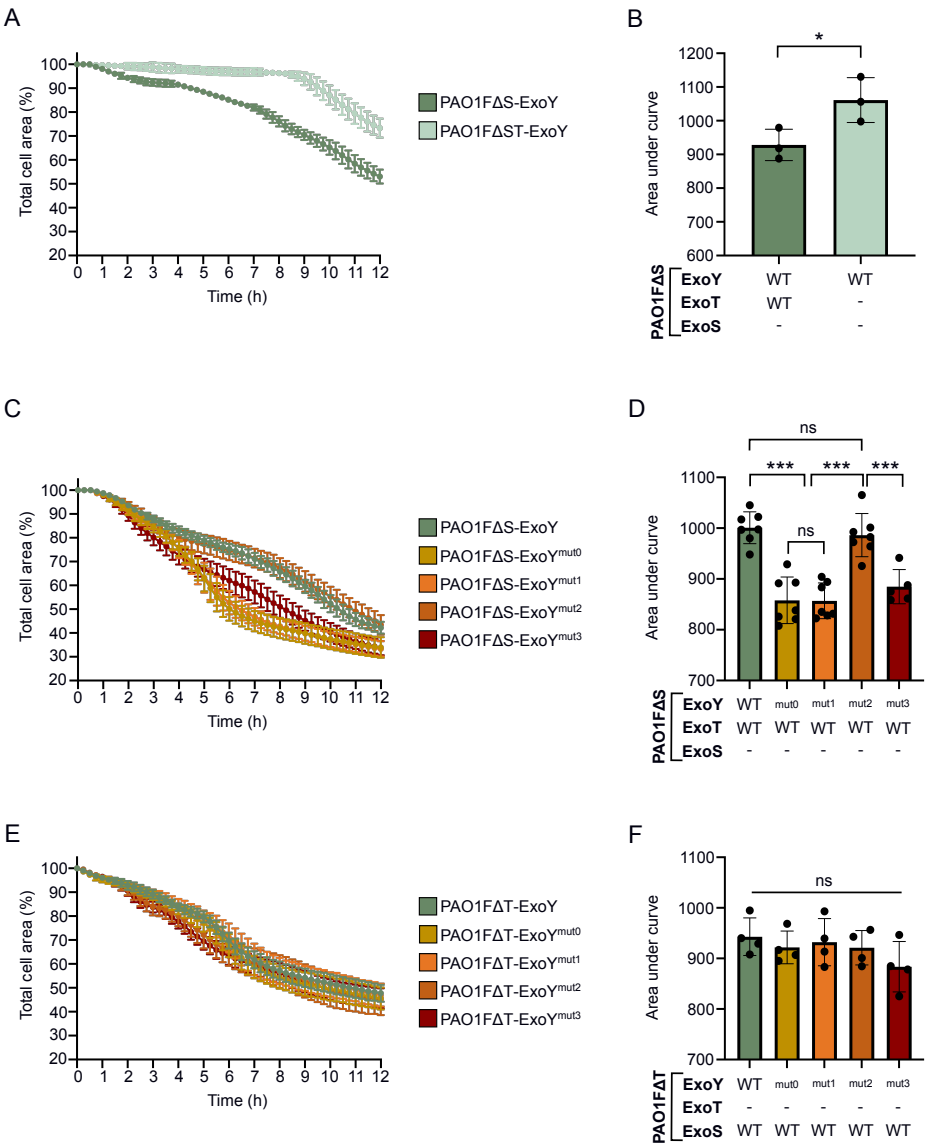

G

pmol/mg of protein	Average level of cGMP in cells after 5h of infection					
	NI	ExoY^{mut0}	ExoY	ExoY^{mut1}	ExoY^{mut2}	ExoY^{mut3}
PAO1FΔS	10 ± 8	5 ± 2	3543 ± 1898	5 ± 2	3545 ± 1929	8 ± 3
PAO1FΔT	9 ± 10	4 ± 3	124 ± 122	4 ± 3	4 ± 3	3 ± 1

Figure 2: Production of cGMP by ExoY alters ExoT cytotoxicity but not ExoS cytotoxicity in NCI-H292 cells.

A. Cell retraction over time in infected NCI-H292 cells. Cells were infected with PAO1FΔS strains injecting ExoY with or without ExoT. Intoxication was quantified every 15 min by time-lapse microscopy. Error bars indicate SD. **B.** Cytotoxicity level of PAO1FΔS strains. The area under the curve (AUC) for each infection curve was plotted. Lower AUCs correspond to higher cytotoxicity. Each dot represents a separate cell retraction assay. The statistical difference was calculated with an unpaired two-tailed t-test *$p < 0.05$. **C.** ExoT-induced cell retraction over time in NCI-H292 cells. Cytotoxicity assay was similar to **A.**, but cells were infected with PAO1FΔS strains co-injecting ExoT with an ExoY variant. **D.** Cytotoxicity level of ExoT-expressing

strains. Representation is similar to **B.** but using the infection assays with PAO1FΔS strains. **E.** ExoS-induced cell retraction over time on NCI-H292 cells. Cytotoxicity assay was similar to **A.** and **C.**, but cells were infected with PAO1FΔT strains co-injecting ExoS with an ExoY variant. **F.** Cytotoxicity level of ExoS-expressing strains. Representation is similar to **B.** and **D.** but using the infection assays with PAO1FΔT strains. Statistical differences were established by one-way ANOVA, followed by Tukey's test (***$p < 0.001$, n.s., non-significant). **G.** Comparative table of intracellular cGMP production after infection of NCI-H292 cells with PAO1FΔS or PAO1FΔT strains. For both conditions, cells were infected for 5h at MOI 20. Intracellular cGMP production was quantified using ELISA kit. Values obtained for PAO1FΔS strains have been extracted from Figure 1H. The mean cGMP accumulation of each sample is shown, together with the SD.

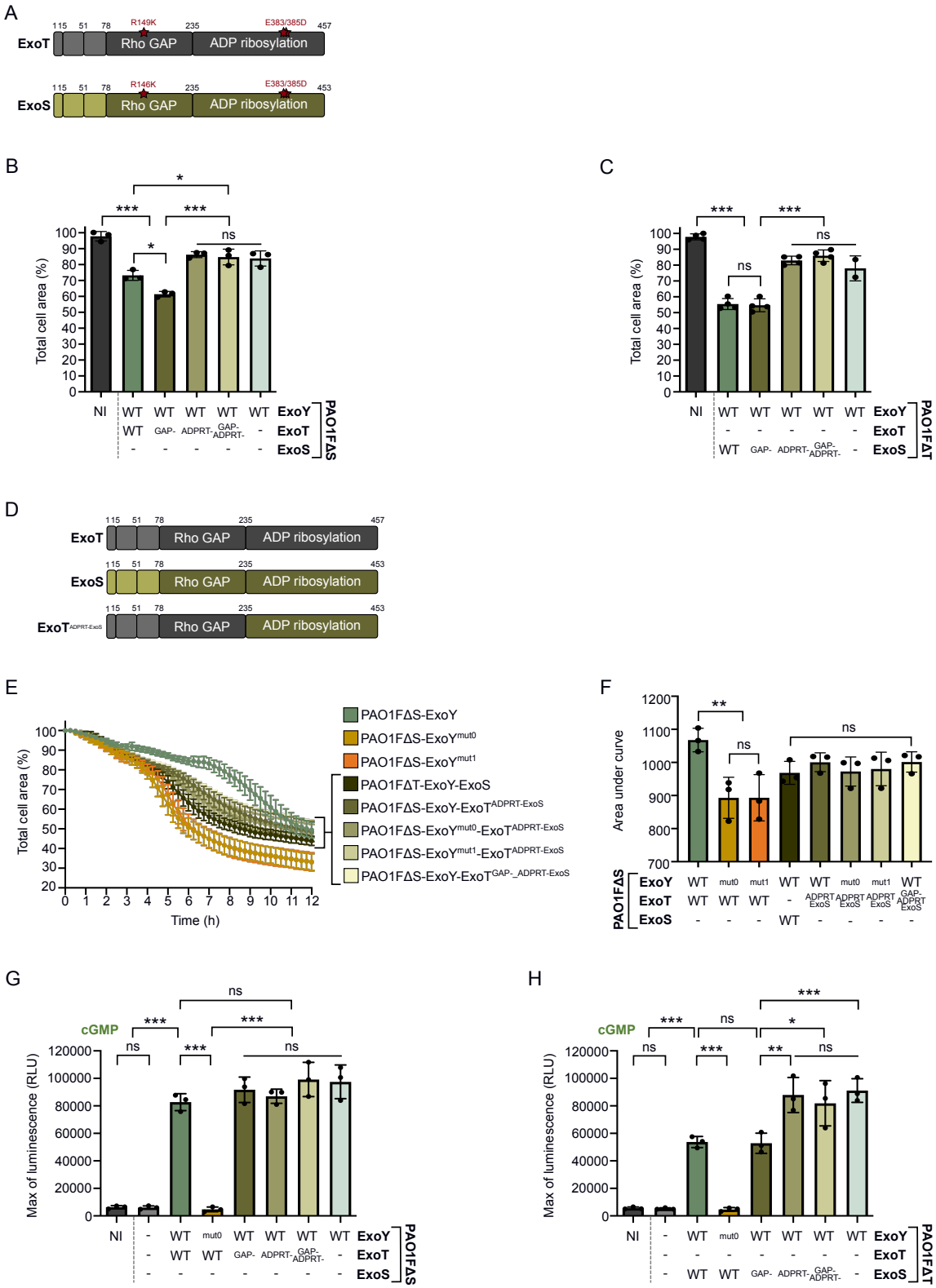

Figure 3: The antagonistic effect of ExoY cGMP production on ExoT cytotoxicity depends on ExoT's ADPRT activity in NCI-H292 cells.

A. Substitutions performed on *exoT* and *exoS* genes to inactivate their GAP and/or ADPRT activity. **B.** Quantification of cell retraction induced by ExoT toxin or its derivatives. Cells were infected at MOI 50 for 8h. Values indicate the percentage of total cell surface after infection

compared with the surface area before infection (T 0h set to 100%). Each data point represents the average value of 16 pictures. **C.** Quantification of cell retraction induced by ExoS toxin or its derivatives. Representation is similar to **B.**, but cells were infected at MOI 20. **D.** Representation of ExoT, ExoS and modified ExoT toxins with their respective GAP and ADPRT domains. In the modified ExoT toxin (chimeric toxin), the ADPRT domain of ExoT has been replaced by that of ExoS to form the $ExoT^{ADPRT\text{-}ExoS}$ toxin. **E.** Infection assay of NCI-H292 cells with PAO1FΔS strains co-injecting ExoT WT or $ExoT^{ADPRT\text{-}ExoS}$ with different ExoY variants (ExoY WT, $ExoY^{mut0}$ and $ExoY^{mut1}$). Error bars indicate SD. **F.** Cytotoxicity level of strains expressing ExoT WT or modified toxin. The area under the curve (AUC) for each infection curve was plotted on a bar graph. Each dot represents a separate cell retraction assay. **G.** Luminescence activity of the cGMP-GloSensor reporter cell line. Cells were infected for 2h at MOI 20 with PAO1FΔS strains co-injecting ExoY with ExoT WT or its inactive mutants prior recording luminescence intensity. The luminescence maximum was extracted and plotted. **H.** Similar to **G.** but cells were infected with PAO1FΔT strains co-injecting ExoY with ExoS WT or its inactive mutants. Statistical differences were established by one-way ANOVA, followed by Tukey's test (*$p = 0.033$, **$p = 0.002$, ***$p < 0.001$, n.s., non-significant).

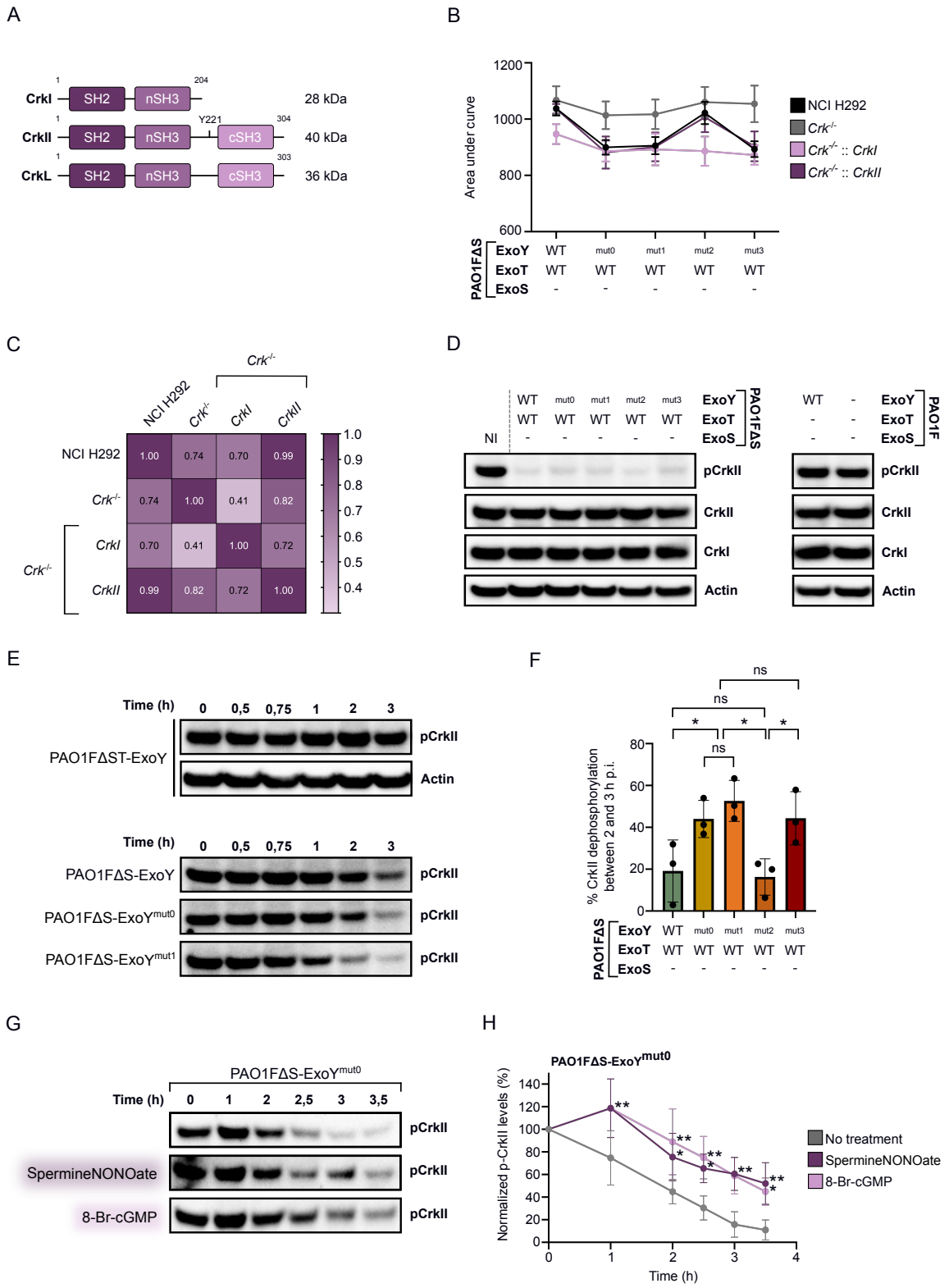

Figure 4: ExoY cGMP production limits ExoT-induced CrkII dephosphorylation in NCI-H292 cells.

A. Representation of CrkI, CrkII and CrkL proteins with their respective Src homology 2 and 3 domains (SH2 and SH3 respectively). The phosphorylation site on CrkII (Y221) is indicated. **B.** Infection profile of NCI-H292 cells and Crk-deficient or complemented cells. Cell retractions were recorded after 12 hours of infection and the AUC of each cell retraction curve was plotted

on the bar chart. For each cell line, the dots were connected to represent the infection profile. Values correspond to averages of five experiments. Error bars indicate SD. **C.** Person correlation between infection profiles of each cell lines. **D.** Western blot (WB) analysis showing levels of CrkI, CrkII and phosphorylated CrkII (Y221) in infected NCI-H292 cells. Cells were infected with the strains for 4h. PAO1FΔST and PAO1FΔSTY strains, injecting only ExoY or no T3SS effector respectively, were also used as controls. **E.** WB analysis of phosphorylated CrkII protein (at Y221) over time in infected cells. NCI-H292 cells were infected for the indicated time with strains injecting or not ExoT together with an ExoY variant. **F.** CrkII dephosphorylation observed between 2- and 3-hours post-infection. Phospho-CrkII (Y221, p-CrkII) levels were normalized to actin levels (loading control) and p-CrkII before infection (Time 0h) was set to 100% to determine the percentage of p-CrkII remaining at 2 and 3h post infection. Statistical differences were established by one way ANOVA, followed by Fisher's LSD test (*$p = 0.033$, **$p = 0.002$, ***$p < 0.001$, n.s., non-significant). **G.** WB analysis of phosphorylated CrkII protein over time in infected NCI-H292 cells supplemented or not with compounds that stimulate cGMP production. SpermineNONOate (50 µM) or 8-Br-cGMP (500 µM) were added in infection medium. **H.** p-CrkII levels over time after infection with PAO1FΔS-ExoY^{mut0} strain. The pCrkII level for each infection time was normalized by actin and compared to the uninfected condition (set at 100%). Statistical differences were established by two ways ANOVA, followed by Dunnett's multiple comparison test with no treatment as the control group (*$p = 0.033$, **$p = 0.002$, n.s., non-significant)

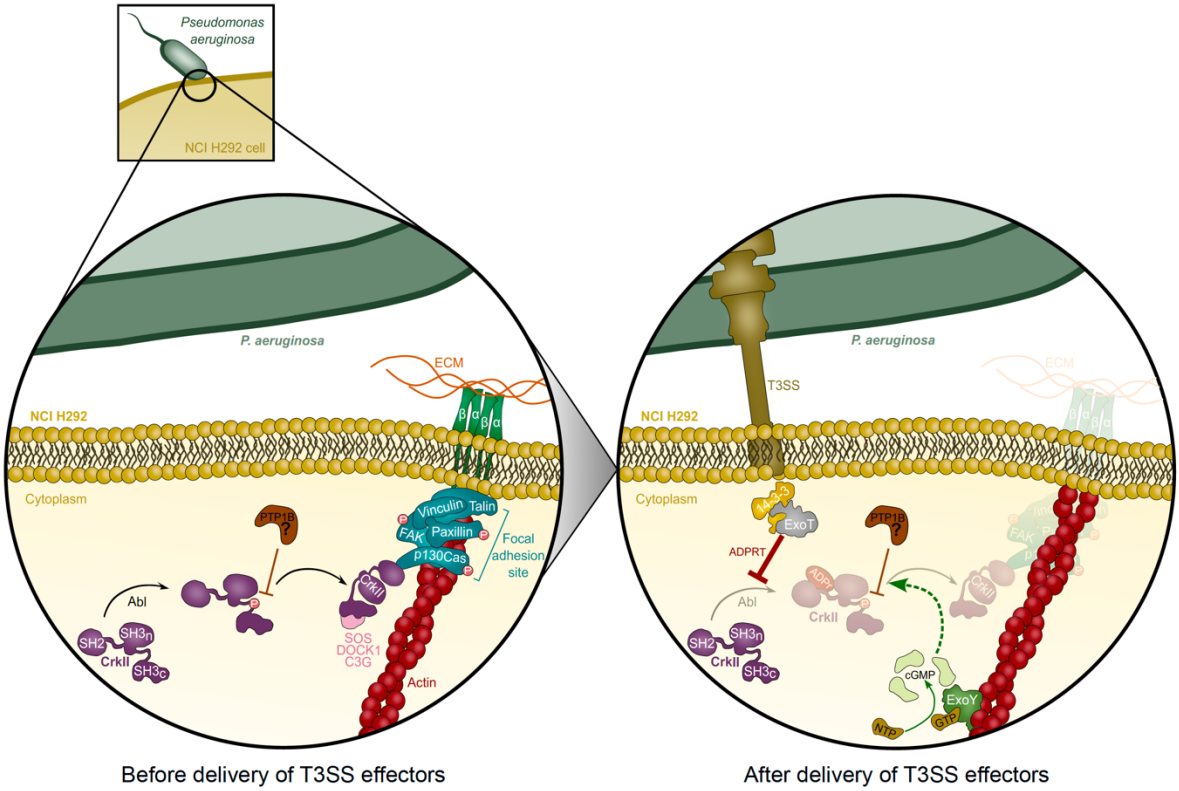

Figure 5: Proposed model of the interplay between ExoY cGMP production and ExoT ADPRT activity in NCI-H292 cells.

Prior to infection, CrkII is phosphorylated by Abl to localize to focal adhesion sites where the adaptor protein is dephosphorylated by a still unknown phosphatase, potentially PTP1B, to interact with tyrosine-phosphorylated p130cas and other partners.

Upon delivery of ExoT and ExoY to the cell cytoplasm by T3SS, ExoY binds to F-actin to become activated and produce cNMPs, primarily cGMP. At the same time, the ADPRT domain of ExoT is activated by the interaction of ExoT with cytoplasmic 14-3-3 proteins. Active ExoT ADP-ribosylates CrkII, which prevents its interaction with Abl (red line) and thus the phosphorylation of CrkII by Abl. This in turn prevents the localization of CrkII to the membrane. Whether the prevention of CrkII phosphorylation by ExoT is sufficient to explain the rapid dephosphorylation of the protein is currently unknown. In addition, the ADPRT domain of ExoT could indirectly lead to the dephosphorylation of CrkII by a mechanism involving the activation of PTPB1 or another phosphatase (dotted red arrow). In either case, dephosphorylation and ADP-ribosylation of CrkII prevent the interaction between CrkII and downstream signaling molecules, thereby disrupting focal adhesion sites, and eventually leading to a programmed apoptotic cell death called anoikis, which involves the loss of interaction with the ECM. However, the production of cGMP by ExoY limits the dephosphorylation of CrkII observed in the presence of ExoT, as suggested by the WB analysis of p-CrkII. This limitation could be due to inhibition of ADPRT activity on the Abl/CrkII interaction and/or on the dephosphorylation by the unknown enzyme (dotted green arrows). Therefore, cGMP production by ExoY attenuates ExoT cytotoxicity and thus regulates *P. aeruginosa* virulence.

Abl: Abelson's tyrosine-protein kinase, PTP1B: protein-tyrosine phosphatase 1B, T3SS: Type 3 Secretion System, cNMPs: cyclic nucleotide monophosphates, ADPRT: ADP-ribosyltransferase domain, p-CrkII: phosphorylated CrkII, ECM: extracellular matrix.

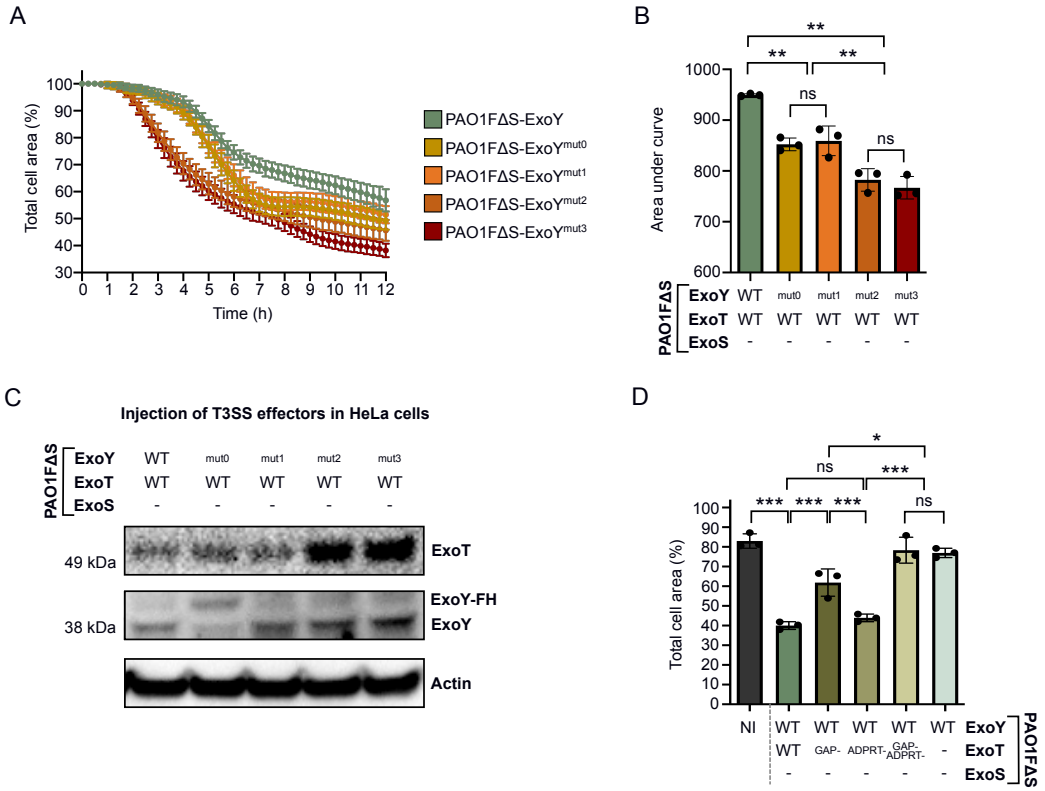

Figure 6: Infection of HeLa cells with PAO1FΔS strains.

A. ExoT-induced cell retraction over time in HeLa cells. The results are presented as the mean percentage (±SD) of the total cell area in comparison to the area before infection. **B.** Cytotoxicity level of ExoT-expressing strains on HeLa cells. The area under the curve (AUC) for each infection curve was plotted and each dot represents a separate cell retraction assay. **C.** Western blot of injected T3SS effectors after infection of HeLa cells with PAO1FΔS strains. Cells were infected for 4h. The ExoY^{mut0} variant in the PAO1FΔS strain has a higher molecular weight because it contains a Flag-His tag at its C-terminus. **D.** Quantification of total cell area of infected HeLa cells. Cells were infected at MOI 50 with PAO1FΔS strains co-injecting ExoY WT with ExoT WT or its inactive mutants. Values indicate the percentage of total cell surface after 10h of infection as compared to the surface before infection (T 0h set to 100%). Each point represents the average value of 17 pictures. Statistical differences were established by one-way ANOVA, followed by Tukey's test (*p = 0.033, **p = 0.002, ***p < 0.001, n.s., non-significant).

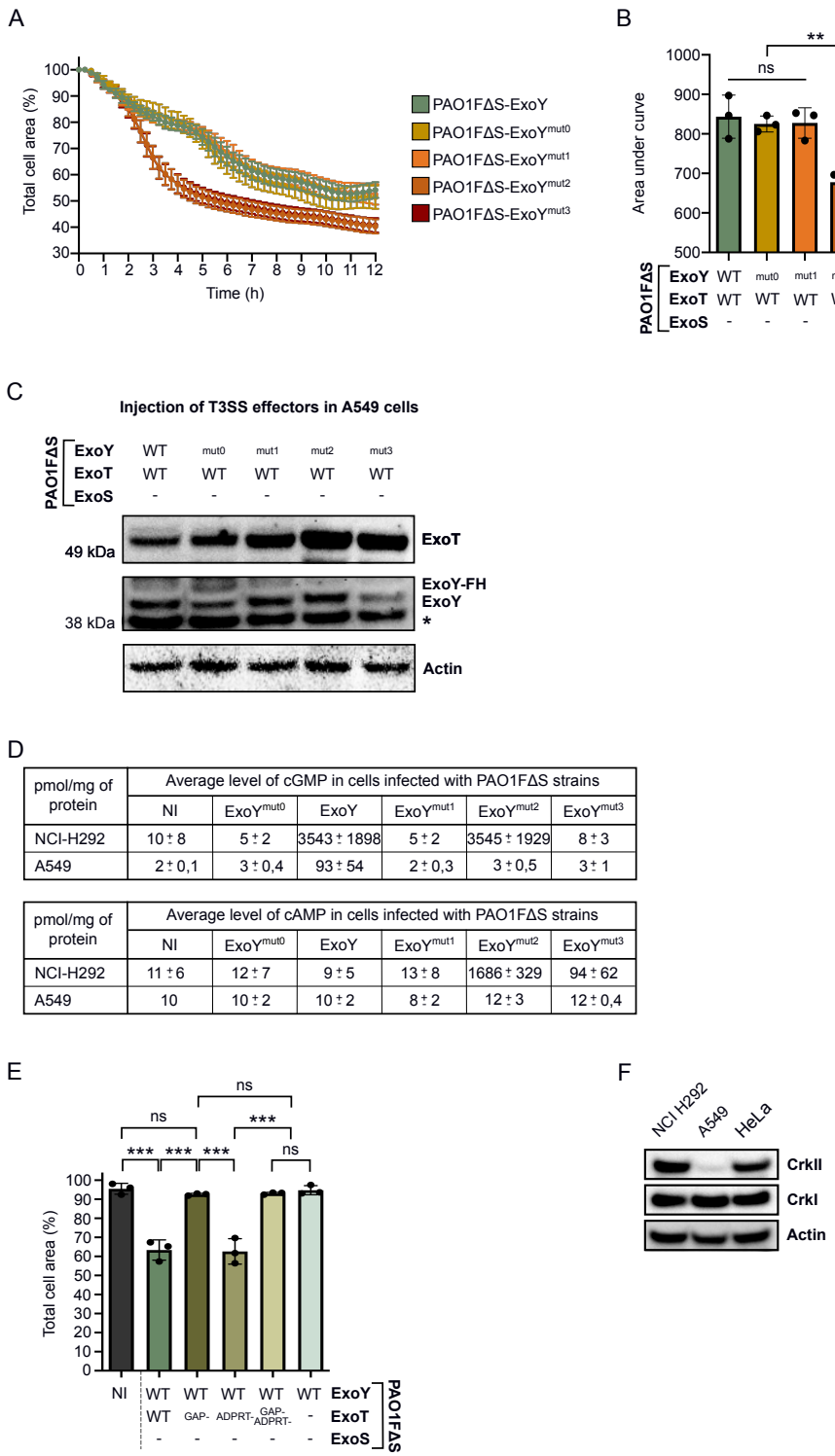

pmol/mg of protein	Average level of cGMP in cells infected with PAO1FΔS strains					
	NI	ExoY^{mut0}	ExoY	ExoY^{mut1}	ExoY^{mut2}	ExoY^{mut3}
NCI-H292	10 ± 8	5 ± 2	3543 ± 1898	5 ± 2	3545 ± 1929	8 ± 3
A549	2 ± 0,1	3 ± 0,4	93 ± 54	2 ± 0,3	3 ± 0,5	3 ± 1

pmol/mg of protein	Average level of cAMP in cells infected with PAO1FΔS strains					
	NI	ExoY^{mut0}	ExoY	ExoY^{mut1}	ExoY^{mut2}	ExoY^{mut3}
NCI-H292	11 ± 6	12 ± 7	9 ± 5	13 ± 8	1686 ± 329	94 ± 62
A549	10	10 ± 2	10 ± 2	8 ± 2	12 ± 3	12 ± 0,4

Figure 7: Infection of A549 cells with PAO1FΔS strains.
A. ExoT-induced cell retraction over time on A549 cells. Cells were infected at MOI of 10 with PAO1FΔS strains. The results are presented as the mean percentage (±SD) of the total cell area in comparison to the area before infection. **B.** Cytotoxicity level of ExoT-expressing strains on A549 cells. The area under the curve (AUC) for each infection curve shown in **A.** was calculated and plotted. Each dot represents a separate cell retraction assay. **C.** Western blot (WB) showing injected T3SS effectors in A549 cells. Cells were infected with PAO1FΔS strains at MOI 10 for 4h. The ExoY^{mut0} variant in the PAO1FΔS strain has a higher molecular weight because it

contains a Flag-His tag at its C-terminus. (*) represents a non-specific band corresponding to a cellular protein that reacts with our ExoY antibody. **D.** Comparative table of intracellular cGMP and cAMP production after infection of NCI-H292 and A549 cells with PAO1FΔS strains. NCI-H292 and A549 cells were infected for 5h at MOI 20 and for 4h at MOI 10, respectively. Intracellular cGMP and cAMP productions were quantified using ELISA kits. Values obtained for NCH-H292 cells have been extracted from Figure 1H and 1I. The mean cGMP and cAMP accumulation of each sample is shown, together with the standard deviation. **E.** Quantification of the total cell area of infected A549 cell. Cells were infected at MOI 10 with PAO1FΔS strains co-injecting ExoY WT with ExoT WT or its inactive mutants. Values indicate the percentage of total cell surface after 8h of infection as compared to the surface before infection (T 0h set to 100%). Each point represents the average value of 7 pictures. Statistical differences were established by one way ANOVA, followed by Tukey's test (*$p = 0.033$, **$p = 0.002$, ***$p < 0.001$, n.s., non-significant). **F.** WB analysis comparing the levels of Crk proteins in NCI-H292 cells, A549 cells and HeLa cells.